NAGRA NTB 90-29
SKB TR 90-20
UK DOE WR 90-051

Poços de Caldas Report No. 11

Testing of geochemical models in the Poços de Caldas analogue study

JANUARY 1991

An international project with the participation of Brazil, Sweden (SKB), Switzerland (NAGRA), United Kingdom (UK DOE) and USA (US DOE). The project is managed by SKB, Swedish Nuclear Fuel and Waste Management Co.

NAGRA NTB 90-29
SKB TR 90-20
UK DOE WR 90-051

Poços de Caldas Report No. 11

Testing of geochemical models in the Poços de Caldas analogue study

JANUARY 1991

An international project with the participation of Brazil, Sweden (SKB), Switzerland (NAGRA), United Kingdom (UK DOE) and USA (US DOE). The project is managed by SKB, Swedish Nuclear Fuel and Waste Management Co.

Testing of geochemical models in the Poços de Caldas analogue study.

J. BRUNO[1], J.E. CROSS[2], J. EIKENBERG[3], I.G. McKINLEY[4], D. READ[5], A. SANDINO[1] and P. SELLIN[6]

[1]Department of Inorganic Chemistry, Royal Institute of Technology (KTH), S-100 44 Stockholm, (Sweden).

[2]Chemistry Division, B10.5 Harwell Laboratory, UKAEA, Harwell, Oxon OX11 ORA (U.K.).

[3]Paul Scherrer Institute (PSI), CH-5232 Villigen PSI (Switzerland).

[4]NAGRA, Parkstrasse 23, CH-5401 Baden (Switzerland).

[5]Atkins E S, Woodcote Grove, Ashley Road, Epsom, Surrey, KT22 7NE (U.K.).

[6]Swedish Nuclear Fuel and Waste Management Company (SKB), Box 5864, S-102 48 Stockholm (Sweden).

Abstract

In order to test the geochemical models used in repository performance assessment, modelling groups were provided with selected major element analyses of Poços de Caldas groundwaters and asked to predict 'blind' the solubility, speciation and limiting solid for a number of trace elements. This report documents these predictions and compares them to field analyses. These tests illustrate particular strengths and weaknesses in current models / databases and allow recommendations for amendments / improvements to be made.

Zusammenfassung

Um die geochemischen Modelle zu prüfen, die in der Sicherheitsanalyse der Endlager angewandt werden, wurden an Modellier-Gruppen ausgewählte Hauptkomponenten-Analysen von Poços de Caldas Grundwässern mit dem Ziel abgegeben, die Löslichkeit, Speziation und die massgebenden Feststoffe für eine Anzahl von Spurenelementen "blind" vorherzusagen. Dieser Bericht dokumentiert diese Vorhersagen und vergleicht sie mit Feldanalysen. Diese Prüfungen illustrieren spezielle Stärken und Schwächen in vorhandenen Modellen/Datenbasen und erlauben Empfehlungen für Änderungen und Verbesserungen.

Résumé

Afin de tester les modèles géochimiques utilisés pour l'évaluation des performances de dépôts finals, on a livré à différentes équipes de modéliseurs une sélection d'analyses en éléments majeurs provenant d'eaux souterraines de la mine de Poços de Caldas; puis on leur a demandé pour un certain nombre d'éléments traceurs de faire une prévision "à l'aveuglette" des paramètres de solubilité, spéciation et limite en constituants solides.

Ce rapport présente ces pronostics et les compare avec les analyses de terrain. Ces tests mettent en lumière les points forts et faibles des modèles actuels/banques de données et permettent de formuler des recommandations pour l'introduction de modifications et améliorations.

Preface

The Poços de Caldas Project was designed to study processes occurring in a natural environment which contains many features of relevance for the safety assessment of radioactive waste disposal. The study area, in the State of Minas Gerais, Brazil, is a region of high natural radioactivity associated with volcanic rocks, geothermal springs and uranium ore deposits. It contains two sites of particular interest on which the project work was focussed: the Osamu Utsumi uranium mine and the Morro do Ferro thorium/rare-earth ore body. The first site is notable in particular for the prominent redox fronts contained in the rock, while Morro do Ferro was already well-known as one of the most naturally radioactive locations on the surface of the Earth, owing to the high thorium ore grade and the shallow, localised nature of the deposit.

The features displayed by these two sites presented the opportunity to study a number of issues of concern in repository performance assessment. The four objectives set after the first-year feasibility study were:

1. Testing of equilibrium thermodynamic codes and their associated databases used to evaluate rock/water interactions and solubility/speciation of elements.
2. Determining interactions of natural groundwater colloids with radionuclides and mineral surfaces, with emphasis on their role in radionuclide transport processes.
3. Producing a model of the evolution and movement of redox fronts, with the additional aim of understanding long-term, large-scale movements of trace elements and rare-earths over the front (including, if possible, natural Pu and Tc).
4. Modelling migration of rare-earths (REE) and U-Th series radionuclides during hydrothermal activity similar to that anticipated in the very near-field of some spent-fuel repositories.

The project ran for three and a half years from June 1986 until December 1989 under the joint sponsorship of SKB (Sweden), NAGRA (Switzerland), the Department of the Environment (UK) and the Department of Energy (USA), with considerable support from a number of organisations in Brazil, notably Nuclebrás (now Urânio do Brasil). The first-year feasibility study was followed by two and a half years of data collection and interpretation, focussed on the four objectives above.

This report is one of a series of 15, summarising the technical aspects of the work and presenting the background data. A complete list of reports is given below. Those in series A present data and interpretations of the sites, while those in series B present the results of modelling the data with performance assessment objectives in mind. The main findings of the project are presented in a separate summary (no. 15).

The work presented in this report is a description of the use of the radionuclide and trace element geochemical database to test the thermodynamic models used for performance assessment.

Poços de Caldas Project Report Series

Series A: Data, Descriptive, Interpretation

Report No.	Topic	Authors (Lead in Capitals)
1.	The regional geology, mineralogy and geochemistry of the Poços de Caldas alkaline caldera complex, Minas Gerais, Brazil.	SCHORSCHER, Shea.
2.	Mineralogy, petrology and geochemistry of the Poços de Caldas analogue study sites, Minas Gerais, Brazil. I: Osamu Utsumi uranium mine.	WABER, Schorscher, Peters.
3.	Mineralogy, petrology and geochemistry of the Poços de Caldas analogue study sites, Minas Gerais, Brazil. II: Morro do Ferro.	WABER.
4.	Isotopic geochemical characterization of selected nepheline syenites and phonolites from the Poços de Caldas alkaline complex, Minas Gerais, Brazil.	SHEA.
5.	Geomorphological and hydrogeological features of the Poços de Caldas caldera and the Osamu Utsumi mine and Morro do Ferro analogue study sites, Brazil.	HOLMES, Pitty, Noy.
6.	Chemical and isotopic composition of groundwaters and their seasonal variability at the Osamu Utsumi and Morro do Ferro analogue study sites, Poços de Caldas, Brazil.	NORDSTROM, Smellie, Wolf.
7.	Natural radionuclide and stable element studies of rock samples from the Osamu Utsumi mine and Morro do Ferro analogue study sites, Poços de Caldas, Brazil.	MacKENZIE, Scott, Linsalata, Miekeley, Osmond, Curtis.
8.	Natural series nuclide and rare-earth element geochemistry of waters from the Osamu Utsumi mine and Morro do Ferro analogue study sites, Poços de Caldas, Brazil.	MIEKELEY, Coutinho de Jesus, Porto da Silveira, Linsalata, Morse, Osmond.

Contents

1. Introduction

Chemical thermodynamic models provide two main types of data for repository performance assessment purposes:

i) Solubilities of particular elements or radionuclides, which constrain their maximum concentration in solution and, if solute transport is limited, their maximum rate of release from a solid phase.

ii) Speciation of such elements in solution, which determines the extent to which the dissolved element will interact with solid phases along a transport path.

Application of these models is widespread and a number of different codes are available which perform the calculations required. However, there are two main uncertainties in their use in performance assessment:

i) The databases of thermodynamic constants ("TDBs") needed for such calculations are rather poorly defined. Uncertainties of many orders of magnitude in the equilibrium constants are quite common and, what is more important, key thermodynamic data may be missing from these databases. The solubilities will be overestimated in the case where an important solubility-limiting solid phase is missing and underestimated if a predominant aqueous complex is absent. In any case, the predicted aqueous speciation will be incorrect.

ii) The models assume that the entire groundwater chemical system is at equilibrium. This is, however, not commonly the case in natural water systems (e.g. Lindberg and Runnells, 1984). The reason is mainly because of the slow kinetics of the water/rock and redox reactions at low temperature. This can normally be handled either by incorporating kinetics into the model or by "switching off" particular reactions.

Both the determination of the critical uncertainties in the thermodynamic databases and the application of geochemical knowledge to a particular system to decide which reactions are possible require expertise.

Within the Poços de Caldas project it was intended to test the thermodynamic models (and their associated databases) used for performance assessment. The predicted solubilities could be then compared to the measured trace element concentrations in the particular groundwaters. Furthermore, it was also intended to roughly evaluate trace element speciation directly in the field using ion-exchange techniques (Appendix 3). This made it possible to distinguish whether the predominant complexes were anionic,

cationic or neutral. The experimental information was then compared with the calculated aqueous speciation.

In this approach it should be noted that, although Poços de Caldas groundwaters were particularly suitable for such analysis due to the presence of the ore bodies, it can never be assured that the water has had the time (or the opportunity) to reach saturation. Thus, if predicted solubilities are above or equal to observed concentrations, it still cannot be assured that the model is correct (or that it conservatively overpredicts). Nevertheless, if the predicted solubilities are lower than observed concentrations, then the model is certainly incorrect.

It should be noted that, as a spin-off, such an exercise also provides a useful intercalibration between the thermodynamic models used by different groups.

2. Methodology

This model-testing exercise proceeded in 2 phases. In the first, 4 groups (SKB, KTH, Harwell and Atkins; Table I) were provided with the major element chemistry of water samples from the Morro do Ferro boreholes MF10, MF11 and MF12. In order mainly to compare the databases used, each group was asked to predict the solubility-limiting phase, the saturation concentration and the aqueous speciation at saturation for U, Th, Pb, V, Ni, Sn, Se and Ra in each of these waters. The results of this work are summarised in Appendix 1 but the main conclusions were:

1. The agreement between the calculations performed by the different groups was satisfactory (± 1 logarithmic unit in trace element concentration). In the case of uranium the differences were larger, especially under reducing conditions. This was due to different U(IV) hydrolysis speciation.

2. For the few elements for which analytical data existed, the calculations predicted higher solubilities than those observed.

3. The solubility may not be controlled by pure solid phases (except for U in the reducing zone) and, for example, coprecipitation with ferric (hydr)oxides may be a key process influencing observed concentrations.

4. The quality of the analytical data for both elements and major components needed to be improved. A set of better characterised and consistent groundwaters is required.

5. The following should be considered for the calculation exercise: Al, Cu, Cd, Zn and rare-earths. This is to provide better grounds for comparison with analytical data and identification of key processes.

Five independent groups of modellers participated in the second phase of this exercise (see Table I).

TABLE I
Modellers, database and codes involved in the study.

Modeller	TDB	Code
Patrik Sellin (SKB)	LLNL	EQ3/6
Amaia Sandino (KTH)	SKBU/HATCHES	PHREEQE
Jost Eikenberg (PSI)	PSI	MINEQL
Jacquie Cross (Harwell)	HATCHES	HARPHRQ
David Read (Atkins)	CHEMVAL	PHREEQE

The modellers were provided with the major component composition and master variable values for three selected waters from the Osamu Utsumi Mine and Morro do Ferro analogue sites. The groundwater compositions given in Table II were evaluated and selected by Nordstrom *et al.* (this report series; Reps. 6 and 14). The trace elements (TE) chosen for these calculations included two groups: a) TEs of relevance for high-level nuclear waste management, i.e. U, Th, Pb, Sr and Ni and b) TEs for which there exist good analytical data and which reflect the geochemistry of the sites, i.e. Mn, Al and Zn.

The participants in this exercise were asked to:

1. Establish the individual solubility-limiting phases for each trace element in the particular groundwaters selected (F1, F5:PC-GW-62 and MF12:PC-GW-50, referred to as F1, F5 and MF12 in the text).
2. Calculate the total concentration of the TEs in equilibrium with the selected individual solid phases.
3. Determine the aqueous speciation of the TEs in equilibrium with the solubility-limiting phase.

TABLE II

Major trace element composition and master variable values for three selected waters from the Osamu Utsumi mine and Morro do Ferro analogue study sites.

	F1 selected	F5: PC-GW-62	MF: PC-GW-50
Temperature	22	24	21
pH	4.87	6.39	6.19
Eh (mV)	338	255	212
Alkalinity (mg/L HCO_3^-)	2.0	26.5	22
Element (mg/L)			
Ca	0.47 ± 0.07	15.6	8.48
Mg	0.07	0.145	0.70
Ba	0.125 ± 0.0055	0.105	< 0.001
Na	0.20 ± 0.02	0.612	0.84
K	12.7 ± 0.6	13	11.2
Li	< 0.010	< 0.01	< 0.015
Fe(II)	1.30	9.25	0.74
Fe(tot)	1.33 ± 0.03	9.35	0.79
SO_4	16 ± 0.5	53	9.5
F	0.41 ± 0.102	6.7	5.3
Cl	3 ± 2.4	< 2.0	< 0.10
Br	< 0.005	< 0.05	< 0.050
NO_3	0.04	< 0.10	1.0
HPO_4	< 0.1	< 0.1	< 0.05
B	< 0.015	0.230	–
SiO_2	35 ± 2.1	37	33.4
S^{2-}	–	< 0.001	< 0.001

The exercise was run as a blind prediction modelling and the participants did not have access to any analytical data for the particular TEs.

3. Results and discussion

In this section, the blind model predictions of the participating groups are presented and compared with observed groundwater concentrations, speciation and ambient mineralogy. It should be emphasised that the water analyses discussed here have been performed on samples subject only to 'conventional' filtration (0.45μm) and thus include a colloidal component (Miekeley *et al.*, this report series; Rep. 9). Where appropriate data exist, the possible role of this colloidal component, which is not included in the thermodynamic models, is discussed.

3.1. Uranium

The uranium concentrations predicted by the different groups of modellers are in good agreement (±1 log unit) in spite of the various solid phases chosen as solubility-limiting and the somewhat different aqueous speciation (see Tables III-V). Pitchblende (U_3O_8) is the solid phase which in most cases appears to be solubility-limiting according to the calculations; this is confirmed by the mineralogical observations (Waber *et al.*, this report series; Rep. 2). In the calculations performed by the Atkins group, the waters are oversaturated with respect to zippeite if they are equilibrated with pitchblende; zippeite has not, however, been observed in the field investigations. In the MF12 waters, the PSI results indicate that schoepite is the solubility-limiting phase.

In general, the calculated uranium concentrations in equilibrium with pitchblende are 2 – 3 orders of magnitude larger than those measured (see Figs. 1 – 3). The reason for these discrepancies could be the formation constant for U_3O_8 chosen by the modellers or source-term limits. The solubility of U_3O_8 (α) has been calculated in a range of groundwaters from Poços de Caldas for which uranium data are available. The thermodynamic database used in these calculations is SKBU1, which has been previously validated. (Bruno and Puigdomènech, 1989). In Figure 4, the comparison between the calculated and measured uranium concentrations is shown. There is a good agreement

TABLE III
Results of the solubility calculations of uranium in the F1 groundwater.

Modeller	[U] mol dm^{-3}	Solubility-limiting phase	Aqueous (%) speciation
SKB	$4.9 \cdot 10^{-5}$	$U_3O_8(\alpha)$	UO_2^{2+} (38) UO_2F^+ (19)
KTH	$1.5 \cdot 10^{-8}$	$U_3O_8(\alpha)$	$(UO_2)_4(OH)_7^+$ (28) UO_2OH^+ (23) $(UO_2)_3(OH)_5^+$ (20)
KTH**	$5.5 \pm 0.6 \cdot 10^{-7}$		$(UO_2)_3(OH)_5^+$ (34)
PSI	$6.1 \cdot 10^{-5}$	$U_3O_8(\alpha)$	UO_2^+ (19) UO_2F^+ (16)
Harwell	$4 \cdot 10^{-5}$	$U_3O_8(\alpha)$	$(UO_2)_3(OH)_5^+$ (22) $UO_2CO_3(aq)$ (18) UO_2F^+ (15)
Atkins	$6 \cdot 10^{-6}$	Zippeite*	UO_2F^+ (36) UO_2^{2+} (22)

(*) Zippeite: $Mg_2(UO_2)_6(SO_4)_3(OH)_{10}\ 8H_2O$.
(**) Average calculation of all F1 waters for which there are U data.

TABLE IV
Results of the solubility calculations of uranium in the F5 groundwater.

Modeller	[U] mol dm^{-3}	Solubility-limiting phase	Aqueous (%) speciation
SKB	$9.0 \cdot 10^{-6}$	$U_3O_8(\alpha)$	UO_2F_2 (26) UO_2F^+ (48)
KTH	$1.43 \cdot 10^{-8}$	$U_3O_8(\alpha)$	UO_2CO_3 (67) $UO_2(CO_3)_2^{2-}$ (23)
PSI	$1.8 \cdot 10^{-5}$	$U_3O_8(\alpha)$	UO_2F_2 (44) UO_2F^+ (27)
Harwell	$6 \cdot 10^{-6}$	$U_3O_8(\alpha)$	$UO_2(CO_3)_2^{2-}$ (27) UO_2CO_3(aq) (36) UO_2F_2 (10)
Atkins	$4 \cdot 10^{-6}$	Zippeite	$(UO_2)_2(OH)_3CO_3^-$ (60) $UO_2(HPO_4)_2^{2-}$ (11)

TABLE V
Results of the solubility calculations of uranium in the MF12 groundwater.

Modeller	[U] mol dm^{-3}	Solubility-limiting phase	Aqueous (%) speciation
SKB	$1.3 \cdot 10^{-6}$	$U_3O_8(\alpha)$	UO_2F_2 (31) UO_2F^+ (26)
KTH	$2.9 \cdot 10^{-7}$	$U_3O_8(\alpha)$	UO_2CO_3 (36) UO_2OH^+ (18)
KTH**	$2.45 \pm 2 \cdot 10^{-8}$		
PSI	$3.3 \cdot 10^{-5}$	UO_3 2 H_2O	$(UO_2)_3(OH)_5^+$ (44) UO_2CO_3(aq) (32)
Harwell	$3 \cdot 10^{-5}$	$U_3O_8(\alpha)$	$(UO_2)_3(OH)_5^+$ (31) UO_2CO_3(aq) (18) $UO_2(HPO_4)_2^{2-}$ (16)
Atkins	$1 \cdot 10^{-5}$	Zippeite	$(UO_2)_2(OH)_3CO_3^-$ (33) $UO_2(HPO_4)_2^{2-}$ (50)

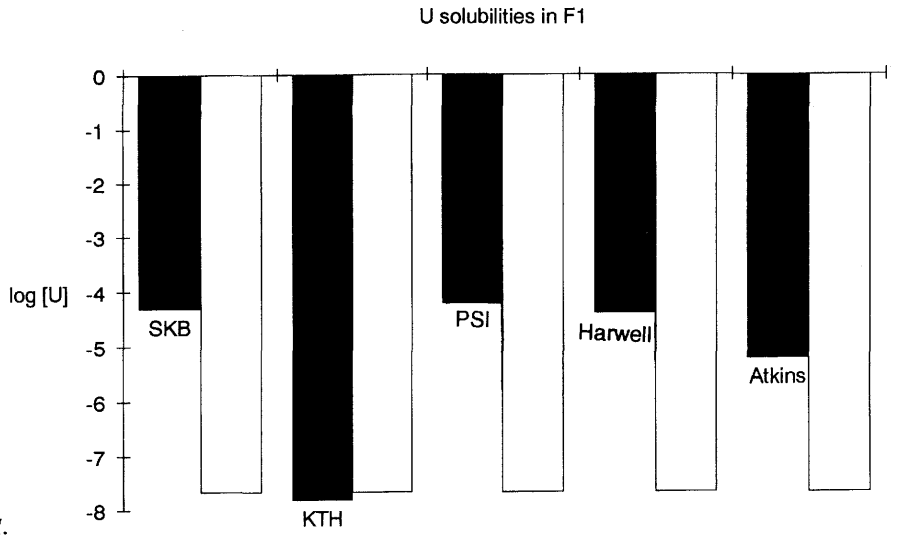

Figure 1.

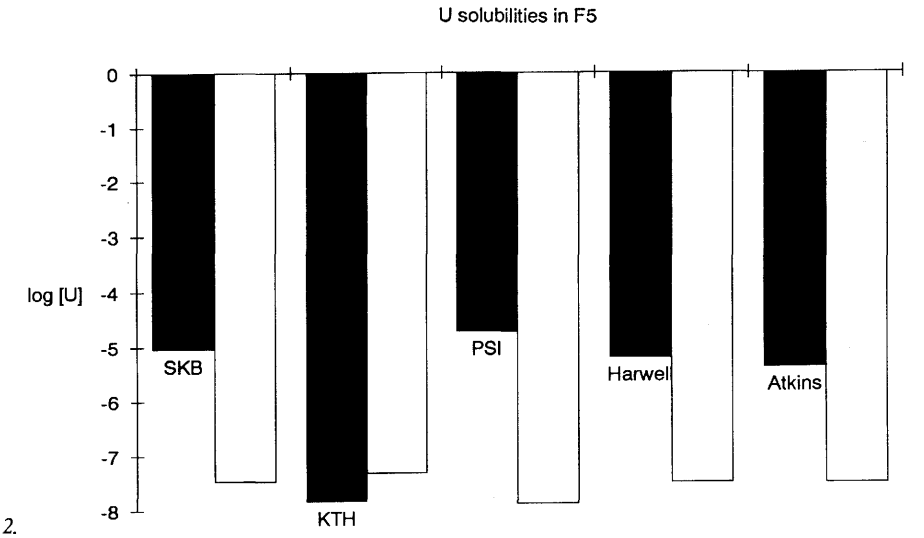

Figure 2.

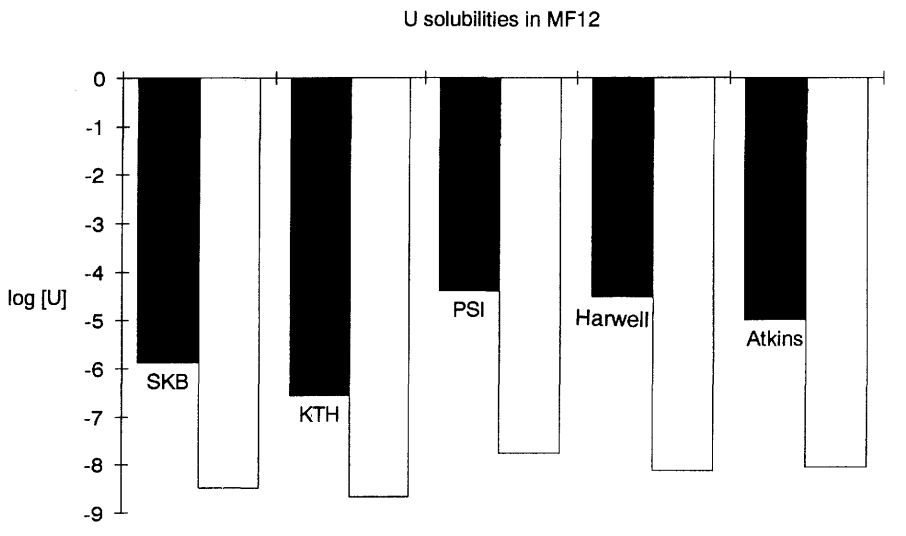

Figure 3.

Figures 1–3. Calculated (black columns) versus measured (white columns) uranium solubilities in the selected F1, F5 and MF12 groundwaters.

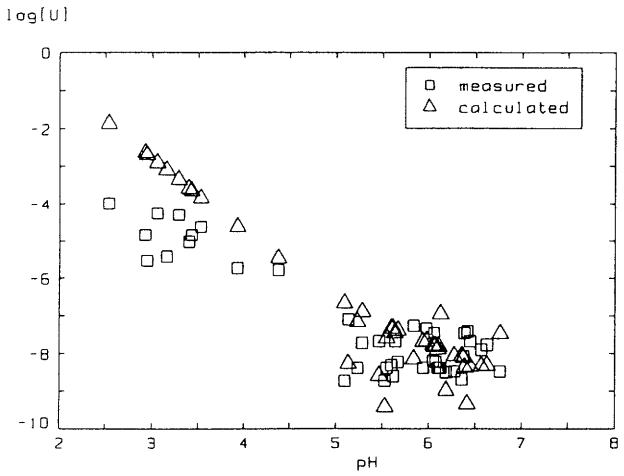

Figure 4.

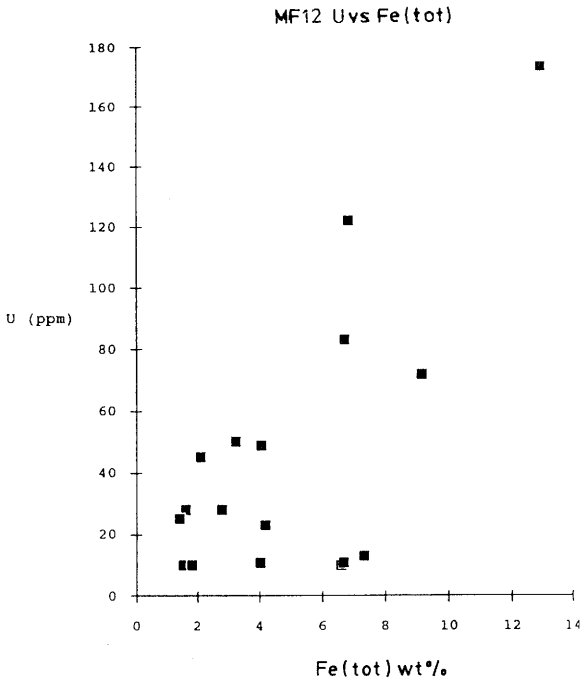

Figure 5.

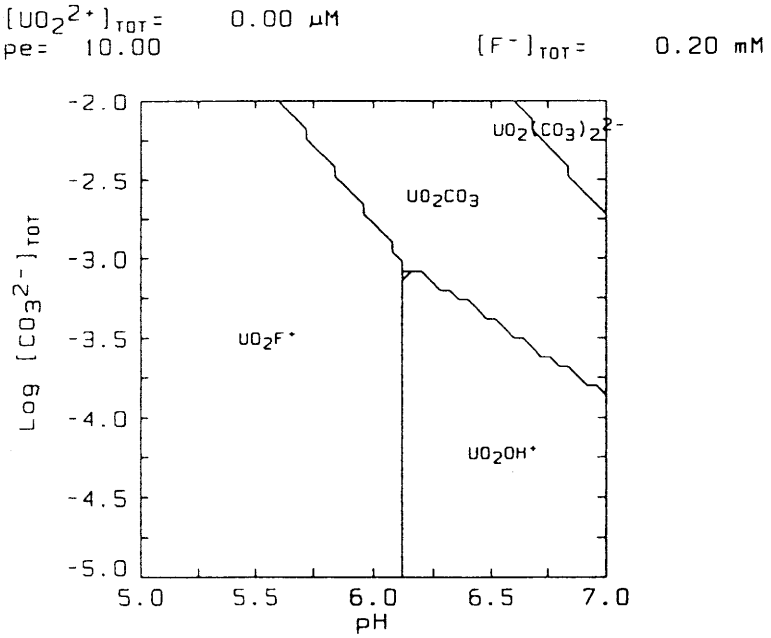

Figure 6.

Figure 4. Calculated uranium solubilities assuming equilibrium with $U_3O_8(c)$ versus measured uranium concentrations as a function of log(U) for all the groundwaters where uranium data were available.

Figure 5. Uranium versus iron content in the parent rock of the MF12 waters.

Figure 6. Predominance diagram of the aqueous uranium speciation in the Poços de Caldas groundwater conditions. (SKBU1 Database).

in the pH range 4.5 to 7 for those groundwaters which are expected to have longer equilibrium times. In the acidic shallow waters, the concentration of uranium appears to be source-term-controlled. The calculated solubilities correspond to a highly crystalline form of pitchblende. The correlation between iron and uranium found in the parent rock at MF12 (Waber, this report series; Rep. 3) implies that uranium is associated with Fe(III)-oxides in the oxidised part of the redox front (see Fig. 5), which may explain why measured concentrations are lower than predicted. This association is further supported by sequential leaching studies (MacKenzie *et al.*, this report series; Rep. 7).

The uranium aqueous speciation is very dependent on the modeller. In F1, the U(VI) speciation is dominated by fluoro complexes in the SKB and Atkins results, while hydroxo complexes are the dominant species for KTH. The results from Harwell indicate that $(UO_2)_3(OH)_5^+$, $UO_2CO_3(aq)$ and UO_2F^+ are equally important. In the F5 groundwater, SKB and PSI predict the formation of U(VI) fluoro complexes, while carbonato complexes are dominant in the calculations by KTH and Harwell. Atkins predicts that the uranium speciation is dominated by $(UO_2)_2(OH)_3CO_3^-$ and $UO_2(HPO_4)^{2-}$. This requires more detailed comment: the stability of the former complex is being re-determined at present at KTH and the results indicate that the actual constant is 0.5 – 1 log units lower (B. Lagerman, personal communication), which has, of course, some influence on its predominance. The existence of $UO_2(HPO_4)^{2-}$ is questionable, as recent solubility measurements at KTH indicate that this complex does not form (Bruno *et al.*, 1990).

The calculated uranium speciation in the MF12 waters varies considerably depending on the modeller. The SKB calculations indicate that fluoro complexes dominate, while for KTH, PSI and Harwell the uranium speciation is divided between hydroxo and carbonato complexes; Atkins calculates the same speciation as in F5 waters.

In general, the differences in the aqueous speciation do not reflect the small variations in the TDBs (see Appendix 2). These are more the result of the different geochemical assumptions made by the modellers and the limitations of particular codes in calculating and keeping constant the given pH. The way the alkalinity was used in the calculations had an important effect on the speciation at these neutral pH values. This is particularly critical in the case of U(VI) speciation in the actual pH ranges considered. Small variations in the pH or total alkalinity of the waters have dramatic effects on the speciation, as is demonstrated in the predominance diagram in Figure 6.

Comparison with results from the field speciation studies at Poços de Caldas, made using the portable column equipment (Appendix 3), does not show a clear picture. According to these field data, the dissolved uranium appears to be associated mainly with

anionic species in the F1 water samples. This is not in agreement with the general speciation trends calculated by the modellers for the F1 groundwater, where UO_2F^+, UO_2^{2+} and $(UO_2)_3(OH)_5^+$ are the dominant species. According to the speciation measurements, the dissolved uranium in the F5 water also appears to be associated with anionic species which, in this case, supports the speciation predicted by KTH, Harwell and Atkins. In the MF12 groundwaters, the speciation measurements show uranium to be divided between anionic, cationic and neutral species. It is therefore very difficult to decide if the calculations are consistent with the results from the column measurements.

Measurements of uranium concentrations in various colloidal fractions from both the Osamu Utsumi mine and Morro do Ferro groundwater samples (Miekeley *et al.*, this report series; Rep. 9) show that most of the uranium is in 'true solution' ($<10^3$ daltons). No measurements were made for F5 samples, but for both F1 and MF12 $\geq 90\%$ of the uranium was in true solution, with most of the balance in the smallest colloidal size fraction ($10^3 - 10^4$ daltons). There is again some evidence of correlation of uranium concentration in colloidal phases with their Fe content, a trend which is even more obvious in the more oxidising, near-surface samples.

3.2. Thorium

The results of the model calculations are shown in Tables VI – VIII, indicating a better agreement among the different model calculations than in the case of uranium. Thorianite (ThO_2) is generally assumed to be the solubility-limiting phase in all groundwaters. The only exception is the PSI group, which predicts $ThF_4(s)$ as the solubility-limiting solid in the F5 groundwater. Thorianite is found as an accessory mineral and is particularly abundant in the ore body at Morro do Ferro. Additional Th-bearing minerals at Morro do Ferro include thorite, cerianite, cheralite and thorbastnaesite, while thorium is also associated with Fe oxyhydroxides and clays in sub-micron particles (Waber, this report series; Rep. 3).

The hypothesis of ThO_2 being the solubility-limiting phase is additionally supported by comparing the measured and calculated solubilities of ThO_2 in the 11 water samples from Poços de Caldas for which Th analyses were available (see Fig. 7). The good agreement between the measured and calculated solubilities in the pH range 4.5 – 7 indicates that thorianite is the solubility-limiting phase for the groundwaters which have had sufficient time to reach equilibrium.

TABLE VI
Results of the solubility calculations of thorium in the selected F1 groundwater.

Modeller	[Th] mol dm^{-3}	Solubility-limiting phase	Aqueous (%) speciation
SKB	$4.9 \cdot 10^{-10}$	$ThO_2(s)$	ThF_2^{2+} (52) $Th(OH)_4$ (19)
KTH	$1.3 \cdot 10^{-9}$	$ThO_2(s)$	$Th(OH)_4$ (63) ThF_4 (18)
PSI	$5.9 \cdot 10^{-10}$	$ThO_2(s)$	$Th(OH)_4$ (42) ThF_2^{2+} (31)
Harwell	$1 \cdot 10^{-7}$	$ThO_2(s)$	$Th(HPO_4)_3^{2-}$ (51) $Th(HPO_4)_2$ (46)
Atkins	$2 \cdot 10^{-7}$	$ThO_2(s)$	$Th(HPO_4)_3^{2-}$ (30) $Th(HPO_4)_2$ (27) ThF_3^{+} (21)

TABLE VII
Results of the solubility calculations of thorium in the F5 groundwater.

Modeller	[Th] mol dm^{-3}	Solubility-limiting phase	Aqueous (%) speciation
SKB	$8.9 \cdot 10^{-9}$	$ThO_2(s)$	ThF_3^{+} (59) ThF_2^{2+} (15)
KTH	$3.6 \cdot 10^{-10}$	$ThO_2(s)$	ThF_4 (29) $Th(OH)_4$ (70)
PSI	$5.8 \cdot 10^{-11}$	$ThF_4(s)$	ThF_3^{+} (50) $ThF_4(aq)$ (27)
Harwell	$2 \cdot 10^{-9}$	$ThO_2(s)$	$Th(HPO_4)_3^{2-}$ (81) $Th(OH)_4$ (12)
Atkins	$2 \cdot 10^{-9}$	$ThO_2(s)$	$Th(HPO_4)_3^{2-}$ (73) $ThF_4(aq)$ (19) ThF_3^{-} (27)

TABLE VIII

Results of the solubility calculations of thorium in the MF12 groundwater.

Modeller	[Th] mol dm^{-3}	Solubility-limiting phase	Aqueous (%) speciation
SKB	$4.3 \cdot 10^{-10}$	$ThO_2(s)$	$Th(OH)_4$ (65) ThF_3^+ (20)
KTH	$9 \cdot 10^{-7}$	$ThO_2(s)$	$Th(HPO_4)_3^{2-}$ (100)
KTH*	$5.2 \cdot 10^{-10}$	$ThO_2(s)$	ThF_4 (50) $Th(OH)_4$ (50)
PSI	$3.1 \cdot 10^{-10}$	$ThO_2(s)$	$Th(OH)_4$ (96)
Harwell	$1 \cdot 10^{-6}$	$ThO_2(s)$	$Th(HPO_4)_3^{2-}$ (100)
Atkins	$1 \cdot 10^{-6}$	$ThO_2(s)$	$Th(HPO_4)_3^{2-}$ (100)
Atkins*	$6 \cdot 10^{-10}$	$ThO_2(s)$	$Th(OH)_4$ (38) ThF_3^+ (33) $ThF_4(aq)$ (26)

(*) no phosphate complexes considered.

In Figures 8 – 10, the predicted thorium concentrations are compared to those measured in the selected groundwaters F1, F5 and MF12. The agreement between the predicted and measured concentrations is amazingly good. Only in the case when phosphate complex formation is assumed are the discrepancies larger. The formation of Th(IV)-phosphate soluble complexes is bound to overestimate thorium solubilities since the phosphate concentrations in the groundwaters are below the detection limit. In addition, the stability of Th-phosphate complexes appears to be greatly overestimated.

In the absence of phosphate complexes the thorium speciation is dominated by the neutral $Th(OH)_4(aq)$ and the positively charged ThF_2^{2+} and ThF_3^+ complexes. This is in agreement with the observations from the speciation columns, where thorium is mainly associated with the cationic resins and gives additional support to the unimportance of the anionic Th(IV)-phosphate complexes.

The analysis of colloids from both Morro do Ferro and the Osamu Utsumi mine (Miekeley *et al.*, this report series; Rep. 9) shows that only ~40% of the <0.45μm filtrate is in true solution, the remnant being fairly evenly distributed between the various colloid size fractions. Even though, on a theoretical basis, very strong thorium complexation with organics would be expected, the correlation of thorium concentration with organic content in the colloid separates is rather weak. This is clearly evident in samples of organic-rich, sub-surface water from Morro do Ferro. There are some indications of correlation of thorium with iron, especially for the more oxidising samples, suggesting

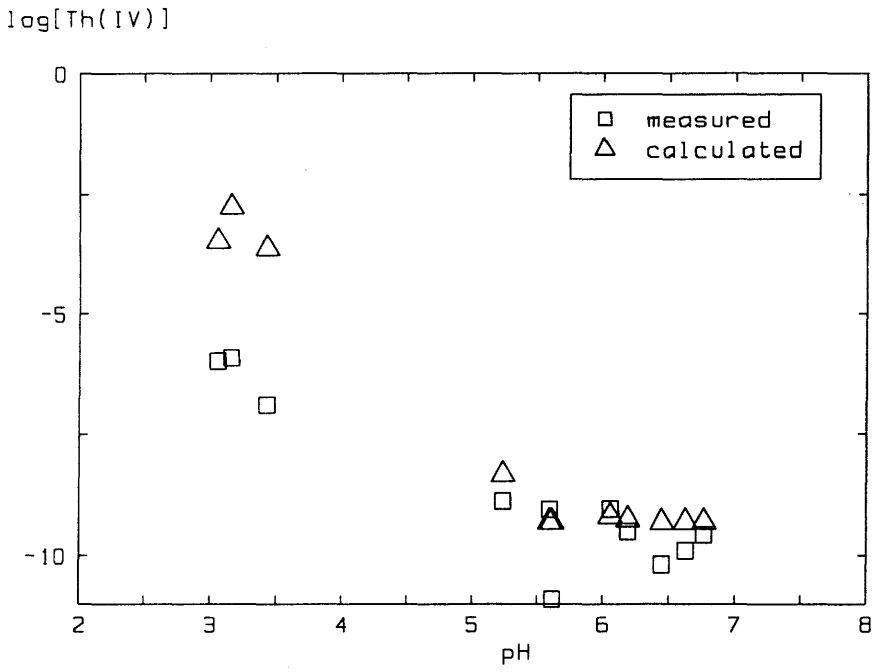

Figure 7. Calculated thorium solubilities assuming equilibrium with $ThO_2(c)$ versus measured thorium concentrations as a function of pH, for all those groundwaters for which thorium data were available.

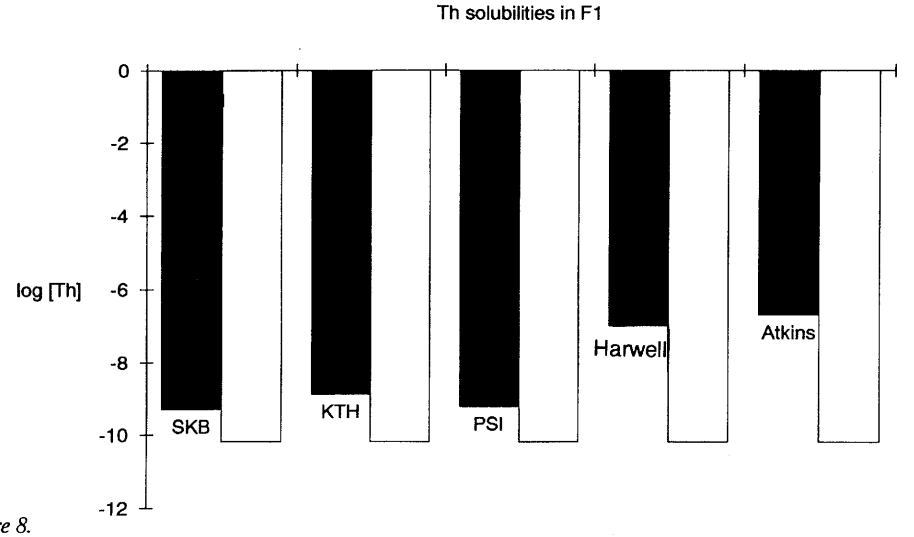

Figure 8.

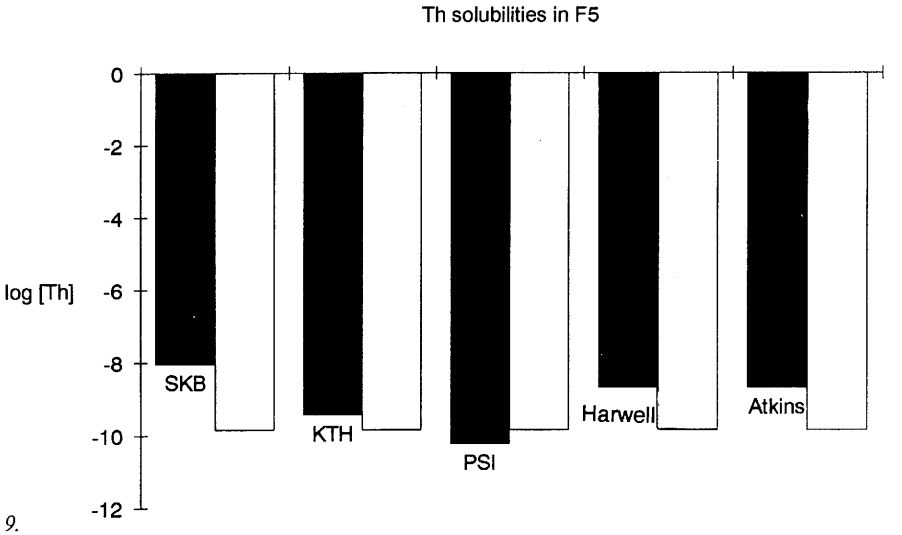

Figure 9.

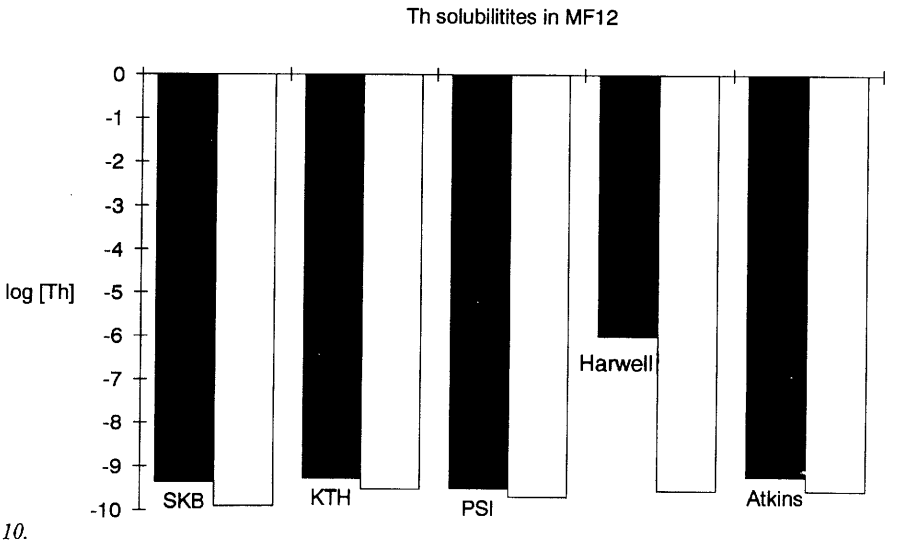

Figure 10.

Figures 8–10. Calculated (black columns) versus measured (white columns) thorium solubilities in the selected F1, F5 and MF12 groundwaters.

uptake by oxyhydroxides. In general, therefore, the colloid analyses support the modelling predictions of predominantly inorganic complexes in these groundwaters.

3.3. Lead

The predicted solubilities of lead in the F1, F5 and MF12 groundwaters are given in Tables IX-XI and it can be seen that those calculated by the different groups agree within about 1 log unit. Cerussite, $PbCO_3$, is the solubility-limiting phase in most of the cases. The SKB results assume the formation of anglesite ($PbSO_4$) in the F1 and F5 groundwaters; this phase is also predicted in the F1 results from the group at Harwell.

The agreement between the predicted Pb(II) solubilities and the measured concentrations is poor in F1 but good in F5 and MF12 (see Figs. 11-13). The low concentrations in F1 probably reflect source-term limitations. This is particularly true in the cases where cerussite is assumed to be the solubility-limiting phase, although there is no indication of the existence of this phase in the mineralogical studies from the boreholes. On the contrary, the whole-rock analysis data show a strong correlation between Pb and P_2O_5 in the oxidised rock at MF12 (see Fig. 14).

The aqueous speciation is dominated by Pb^{2+} and $PbCO_3(aq)$, depending on the pH and alkalinity of the groundwaters.

In both Morro do Ferro and the Osamu Utsumi mine, ~60 – 70% of the lead concentrations in deep waters is in true solution with the balance in colloidal fractions.

TABLE IX
Results of the solubility calculations of lead in the F1 groundwater.

Modeller	[Pb] mol dm^{-3}	Solubility-limiting phase	Aqueous (%) speciation
SKB	$1.2 \cdot 10^{-4}$	$PbSO_4(s)$	$PbCO_3(aq)$ (91)
KTH	$5.4 \cdot 10^{-6}$	$PbCO_3(s)$	$PbCO_3(aq)$ (91)
PSI	$1.1 \cdot 10^{-4}$	$PbSO_4(s)$	Pb^{2+} (95)
Harwell	$1 \cdot 10^{-4}$	$PbSO_4(s)$	Pb^{2+} (90)

TABLE X
Results of the solubility calculations of lead in the F5 groundwater.

Modeller	[Pb] mol dm^{-3}	Solubility-limiting phase	Aqueous (%) speciation
SKB	$2.3 \cdot 10^{-4}$	$PbSO_4(s)$	$PbCO_3(aq)$ (80) Pb^{2+} (20)
KTH	$4 \cdot 10^{-6}$	$PbCO_3(s)$	$PbCO_3(aq)$ (91)
PSI	$2.1 \cdot 10^{-5}$	$PbCO_3(s)$	Pb^{2+} (80) $PbSO_4(aq)$ (15)
Harwell	$6.5 \cdot 10^{-6}$	$PbCO_3(s)$	Pb^{2+} (61) $PbCO_3(aq)$ (24)

TABLE XI
Results of the solubility calculations of lead in the MF12 groundwater.

Modeller	[Pb] mol dm^{-3}	Solubility-limiting phase	Aqueous (%) speciation
SKB	$2.5 \cdot 10^{-4}$	$PbCO_3(s)$	$PbCO_3(aq)$ (91) Pb^{2+} (20)
KTH	$4 \cdot 10^{-6}$	$PbCO_3(s)$	$PbCO_3(aq)$ (91)
PSI	$4.2 \cdot 10^{-6}$	$PbCO_3(s)$	Pb^{2+} (72) $PbCO_3(aq)$ (20)
Harwell	$7.3 \cdot 10^{-6}$	$PbCO_3(s)$	Pb^{2+} (72) $PbCO_3(aq)$ (22)

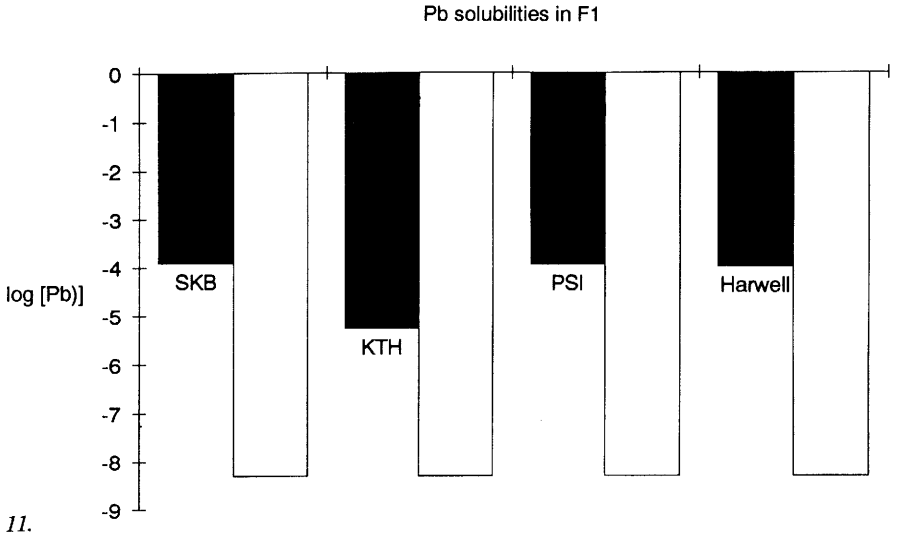

Figure 11.

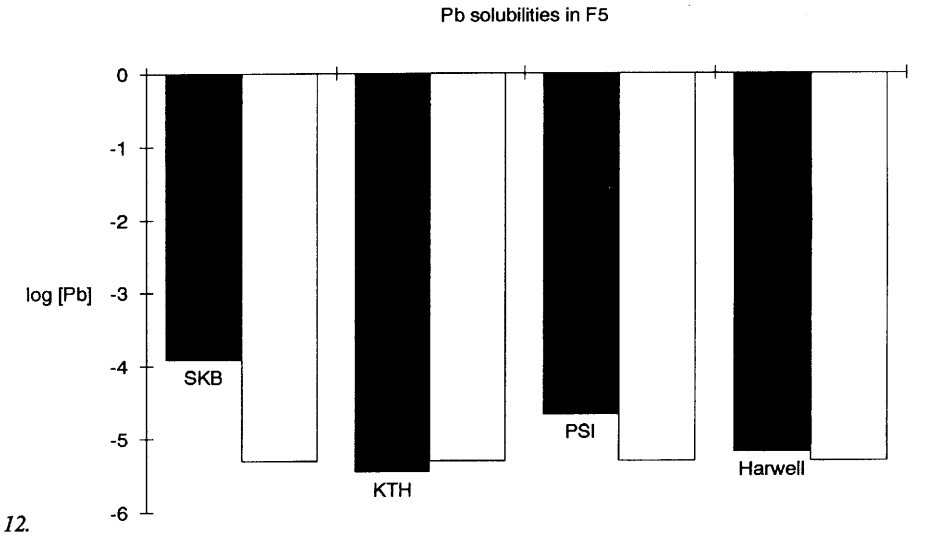

Figure 12.

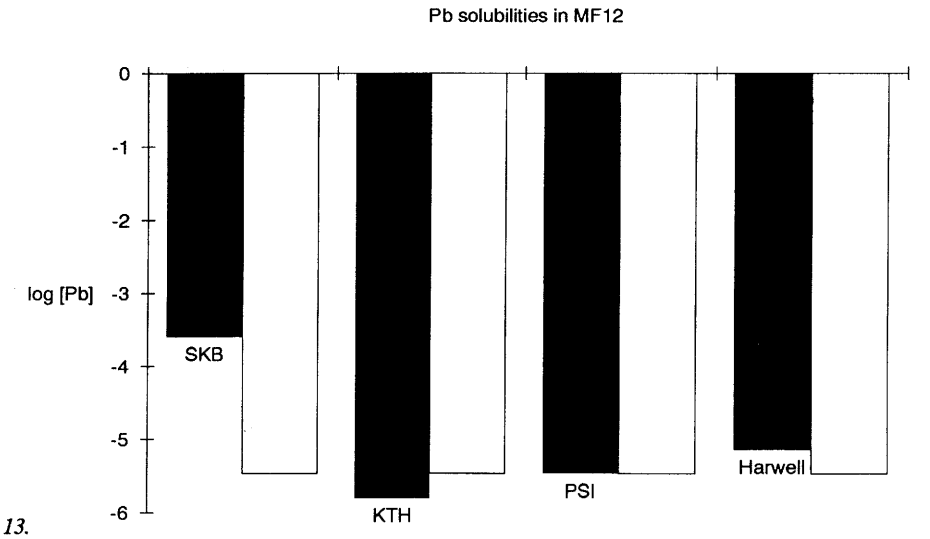

Figure 13.

Figures 11 – 13. Calculated (black columns) versus measured (white columns) lead solubilities in the selected F1, F5 and MF12 groundwaters.

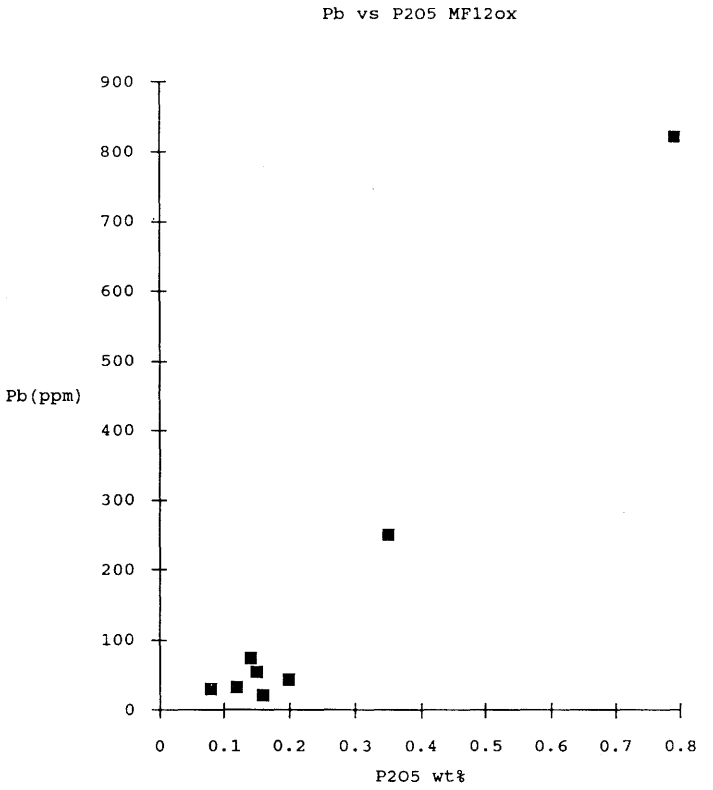

Figure 14. Lead versus P_2O_5 content in the oxidised MF12 host phonolite rock.

Like the other trace elements, it seems probable that lead is associated with organic or iron oxyhydroxide phases in these colloids.

3.4. Nickel

The results are given in Tables XII-XIV and agreement between the different groups is seen to be very poor. The KTH, PSI and Harwell groups assume $Ni(OH)_2(s)$ or $NiO_{(s)}$ to be the solubility-limiting phase, which results in very high Ni(II) concentrations. In the calculations performed by the SKB group, Ni-ferrite ($NiFe_2O_4$-trevorite) is assumed to be the solubility-limiting phase, resulting in calculated solubilities which are 5 to 9 orders of magnitude lower.

The comparison between predicted and measured Ni(II) concentrations is not very encouraging (see Figs. 15-17). The calculated solubility of $Ni(OH)_2(s)/NiO_{(s)}$ in these groundwaters is very high compared to the measured Ni(II) concentrations.

The very low solubilities predicted by consideration of $NiFe_2O_4$ as the limiting solid are, however, far below measured concentrations. This is a clear case where the model prediction is non-conservative; either the $NiFe_2O_4$ data are incorrect (this solid being included in relatively few databases; Baeyens and McKinley, 1989) or, more likely, this solid simply does not form under low-temperature conditions. It should be noted that $NiFe_2O_4$ could be regarded as a 1:1 "solution" of NiO in Fe_2O_3 and the thermodynamic treatment of such mixed systems must be handled very carefully (for discussion see

TABLE XII
Results of the solubility calculations of nickel in the F1 groundwater.

Modeller	[Ni] mol dm^{-3}	Solubility-limiting phase	Aqueous (%) speciation
SKB	$4.9 \cdot 10^{-9}$	$NiFe_2O_4$	Ni^{2+} (98)
KTH	$5.1 \cdot 10^{-2}$	$Ni(OH)_2(s)$	Ni^{2+} (94) $NiCO_3$ (90)
PSI	$9.8 \cdot 10^{-4}$**		$NiCO_3$ (90) $Ni2^+$ (10)
Harwell*	$4.3 \cdot 10^{-4}$	$Ni(OH)_2(s)$	Ni^{2+} (97)

(*) pH drift to 7.1 as a result of HARPHRQ calculations.
(**) pH drift to 8.3 as a result of PHREEQE calculations.

TABLE XIII

Results of the solubility calculations of nickel in the F5 groundwater.

Modeller	[Ni] mol dm^{-3}	Solubility-limiting phase	Aqueous (%) speciation
SKB	$9.2 \cdot 10^{-13}$	$NiFe_2O_4$	Ni^{2+} (96)
KTH	$5.1 \cdot 10^{-2}$	$Ni(OH)_2$	Ni^{2+} (99)
PSI	$2.6 \cdot 10^{-3*}$	NiO	$NiCO_3$ (91) $Ni2^{+}$ (8)
Harwell	$2.3 \cdot 10^{-2}$	$Ni(OH)_2(s)$	Ni^{2+} (93)

(*) pH drift to 8.1 as a result of PHREEQE calculations.

TABLE XIV

Results of the solubility calculations of nickel in the MF12 groundwater.

Modeller	[Ni]mol dm^{-3}	Solubility-limiting phase	Aqueous (%) speciation
SKB	$3.0 \cdot 10^{-14}$	$NiFe_2O_4$	Ni^{2+} (99)
KTH	$5.1 \cdot 10^{-2}$	$Ni(OH)_2$	Ni^{2+} (99)
PSI	$3.6 \cdot 10^{-4*}$	NiO	$NiCO_3$ (89) $Ni2^{+}$ (11)
Harwell	$2.7 \cdot 10^{-2}$	$Ni(OH)_2(s)$	Ni^{2+} (99)

(*) pH drift to 8.1 as a result of PHREEQE calculations.

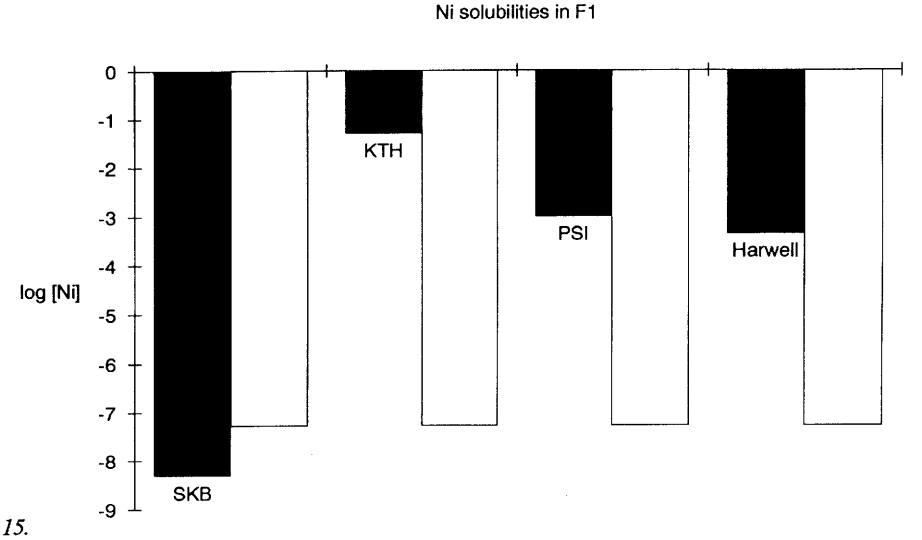

Figure 15.

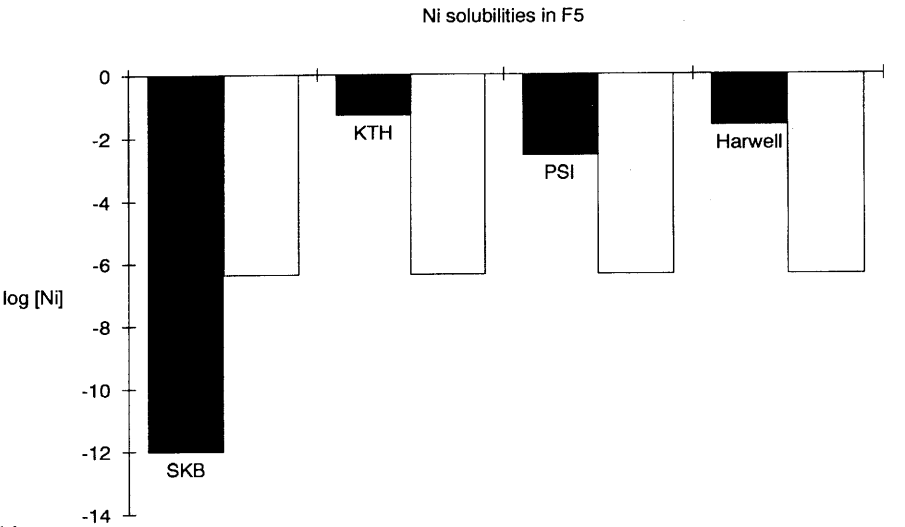

Figure 16.

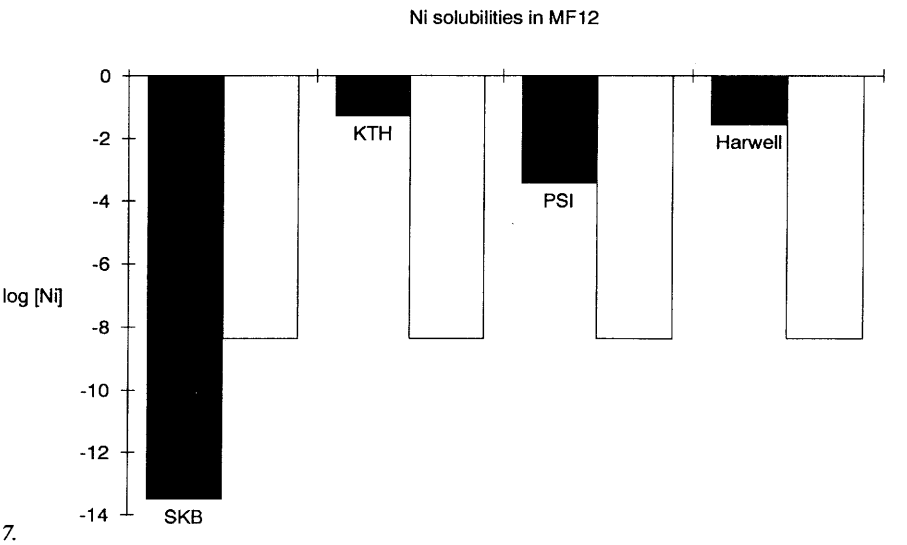

Figure 17.

Figures 15 – 17. Calculated (black columns) versus measured (white columns) nickel solubilities in the selected F1, F5 and MF12 groundwaters.

Schweitzer, 1989). There are, unfortunately, no Ni measurements on colloids but, assuming that Ni follows Fe, one would expect 80 – 90% of the measured concentration to be in true solution. Colloids would not, therefore, provide any explanation for the non-conservatism of this prediction.

It should be emphasised that the observed concentrations of Ni are at, or only slightly above, the detection limit. Whole-rock analysis also indicates very low Ni concentrations at both sites (Waber *et al.*; Waber, this report series; Reps. 2 and 3), except around the redox front, and hence it may be that these groundwaters are source-term-limited. Alternatively, concentrations may be limited by coprecipitation with Fe oxyhydroxides.

The models generally predict Ni^{2+} as the dominant aqueous species. Only PSI predicts an uncharged carbonate species as a result of the pH drift in their calculations. The agreement between the various models probably reflects more the very limited data available rather than consistency between independent data sources (Baeyens and McKinley, 1989).

3.5. Strontium

The results from the solubility-limiting calculations for Sr are given in Tables XV-XVII and the agreement between the Sr solubilities calculated by different groups is seen to be fair. In most cases strontianite ($SrCO_3$) is assumed to be the solubility-limiting phase. The calculations from Harwell assume the formation of $SrHPO_4(s)$, although this does not influence the calculated Sr concentrations which are consistently much higher than those measured (Figs. 18-20). The strong correlation between Sr and P_2O_5 in the parent rock (Fig. 21) could indicate that the solubility of Sr is controlled by some Sr/Ca phosphate solid solution or by minerals such as goyazite ($SrAl_3\,(PO_4)_2\,(OH)_5 \cdot H_2O$), which has been identified at the Osamu Utsumi mine.

According to these calculations, Sr(II) is present as the Sr^{2+} free ion in groundwaters F1, F5 and MF12. In all samples analysed, $\geq$99% of all Sr was present in the 'true solution' phase, indicating very little uptake by either organic or Fe oxyhydroxide colloids. This behaviour generally matches that of the other alkaline earths, although there is a tendency for the lighter members of this series (Ca, Mg) to be associated more with colloids than the heavier Sr and Ba. It may thus be expected that Ra would also show little association with colloids.

TABLE XV

Results of the solubility calculations of strontium in the F1 groundwater.

Modeller	[Sr] mol dm^{-3}	Solubility-limiting phase	Aqueous (%) speciation
SKB	$1.5 \cdot 10^{-2}$	$SrCO_3(s)$	Sr^{2+} (98)
KTH	$2.59 \cdot 10^{-3}$	$SrCO_3(s)$	Sr^{2+} (98)
Harwell	$7 \cdot 10^{-3}$	$SrHPO_4(s)$	Sr^{2+} (99)
Atkins*	$2 \cdot 10^{-4}$	$SrCO_3(s)$	Sr^{2+} (96)

(*) pH drift to 8.8 as a result of PHREEQE calculations.

TABLE XVI

Results of the solubility calculations of strontium in the F5 groundwater.

Modeller	[Sr]mol dm^{-3}	Solubility-limiting phase	Aqueous (%) speciation
SKB	$1.5 \cdot 10^{-2}$	$SrCO_3(s)$	Sr^{2+} (94)
KTH	$9.3 \cdot 10^{-4}$	$SrCO_3(s)$	Sr^{2+} (98)
Harwell	$1 \cdot 10^{-3}$	$SrHPO_4(s)$	Sr^{2+} (91)
Atkins	$5 \cdot 10^{-4}$	$SrCO_3(s)$	Sr^{2+} (90)

TABLE XVII

Results of the solubility calculations of strontium in the MF12 groundwater.

Modeller	[Sr] mol dm^{-3}	Solubility-limiting phase	Aqueous (%) speciation
SKB	$6.8 \cdot 10^{-2}$	$SrCO_3(s)$	Sr^{2+} (99)
KTH	$3.83 \cdot 10^{-3}$	$SrCO_3(s)$	Sr^{2+} (98)
Harwell	$1 \cdot 10^{-3}$	$SrHPO_4(s)$	Sr^{2+} (98)
Atkins*	$2 \cdot 10^{-4}$	$SrCO_3(s)$	Sr^{2+} (96)

(*) pH drift to 8.3 as a result of PHREEQE calculations.

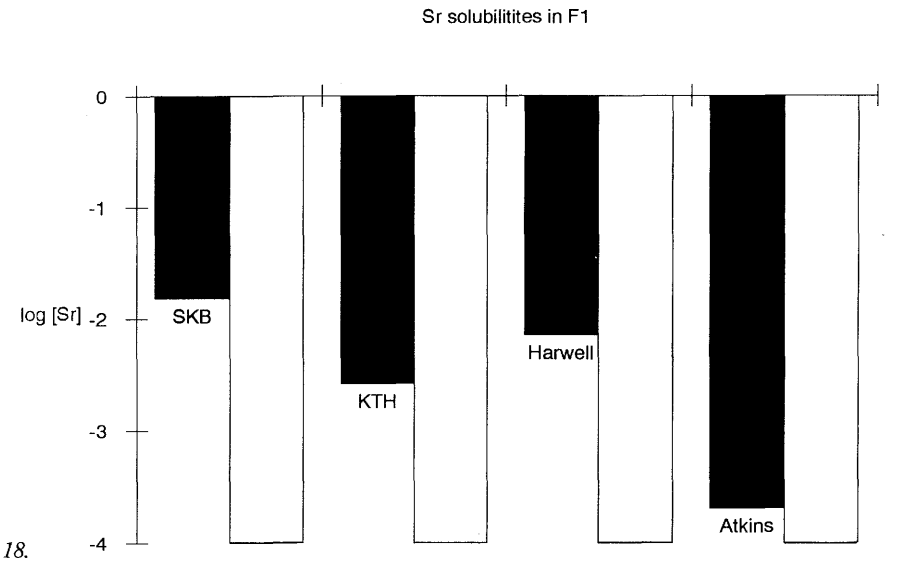

Figure 18.

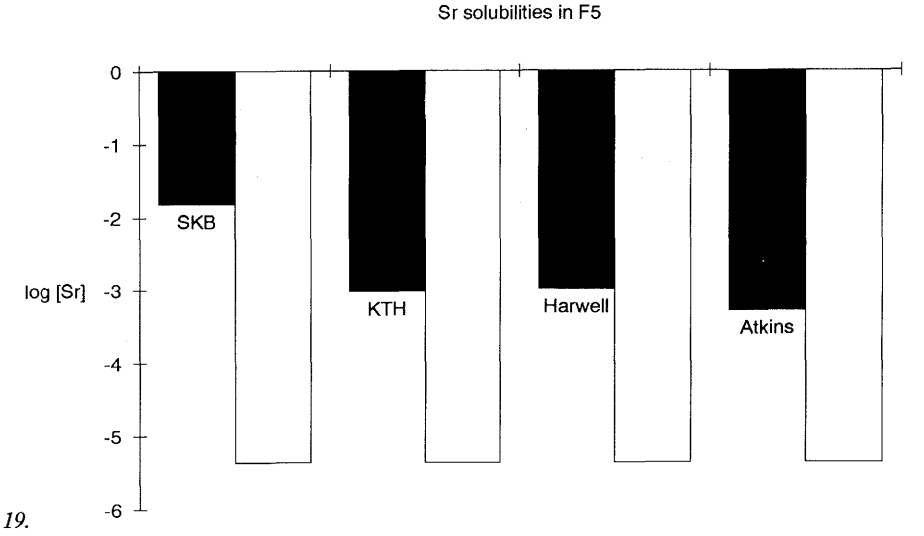

Figure 19.

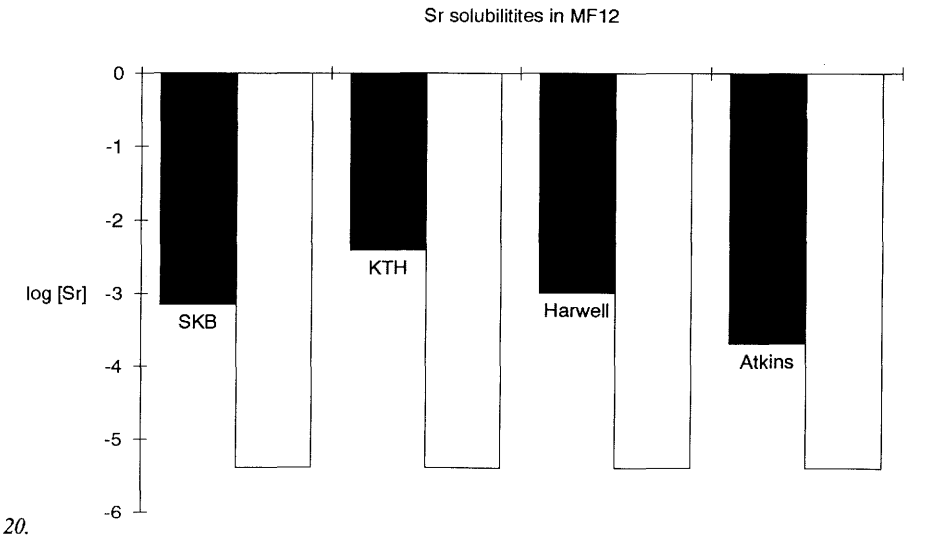

Figure 20.

Figures 18 – 20. Calculated (black columns) versus measured (white columns) strontium solubilities in the selected F1, F5 and MF12 groundwaters.

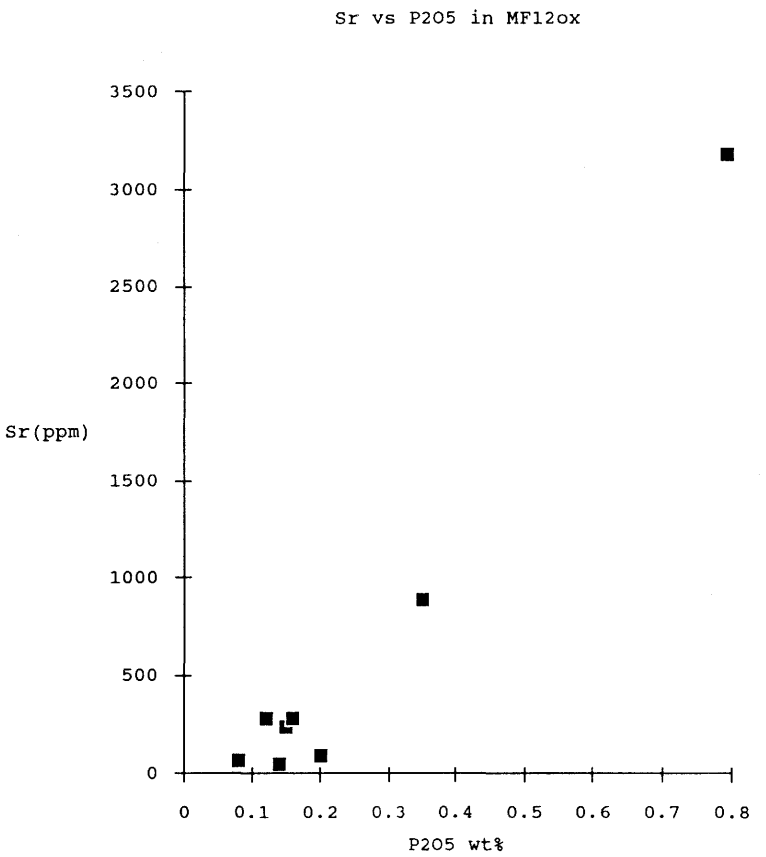

Figure 21. Strontium versus P_2O_5 content in the oxidised MF12 host phonolite rock.

3.6. Vanadium

Vanadium is an interesting trace element because its redox-sensitivity is similar to that of uranium; this accounts for its common association with roll-front uranium ores. The results from the model calculations are shown in Tables XVIII-XX. The vanadium solubilities are rather high if V_2O_4(s) is assumed to be the solubility-limiting phase; this is in fact a stable phase at the pyrite/$Fe(OH)_3$ redox boundary. The calculated solubilities, assuming equilibrium with mixed uranium/vanadium silicate phases (i.e. carnotite and tyuyamunite), are much lower. The predicted vanadium solubilities can only be compared with detection limits as no measurable concentrations were detected in F1, F5 and MF12 groundwaters (see Figs. 22-24). No specific vanadium minerals have been identified for either site and whole-rock vanadium concentrations are fairly consistent (mainly 200–40 ppm), indicating low mobility of this element (Waber *et al.*, this report series; Rep. 2).

The aqueous speciation is predicted to be dominated by the $VO_2(OH)_2^-$ at low concentrations (Baes and Mesmer, 1976). Vanadium was not analysed in the colloid separates.

TABLE XVIII
Results of the solubility calculations of vanadium in F1 groundwater.

Modeller	[V] mol dm^{-3}	Solubility-limiting phase	Aqueous (%) speciation
SKB	$5.4 \cdot 10^{-9}$	Carnotite	$VO_2(OH)_2^-$ (73) VO^{2+} (14)
Harwell	$4.4 \cdot 10^{-5}$	V_2O_4	$VO_2(OH)_2^-$ (79)

Carnotite: $K_2(UO_2)_2(VO_4)_2$.

TABLE XIX
Results of the solubility calculations of vanadium in the F5 groundwater.

Modeller	[V] mol dm^{-3}	Solubility-limiting phase	Aqueous (%) speciation
SKB	$1.6 \cdot 10^{-8}$	Tyuyamunite	$VO_2(OH)_2^-$ (91)
Harwell	$1.6 \cdot 10^{-3}$	V_2O_4	$VO_2(OH)_2^-$ (99)

Tyuyamunite: $Ca(UO_2)_2(VO_4)_2$.

TABLE XX
Results of the solubility calculations of vanadium in the MF12 groundwater.

Modeller	[V] mol dm^{-3}	Solubility-limiting phase	Aqueous (%) speciation
SKB	$1.4 \cdot 10^{-8}$	Tyuyamunite	$VO_2(OH)_2^-$ (91)
Harwell	$9.1 \cdot 10^{-3}$	V_2O_4	$VO_2(OH)_2^-$ (99)

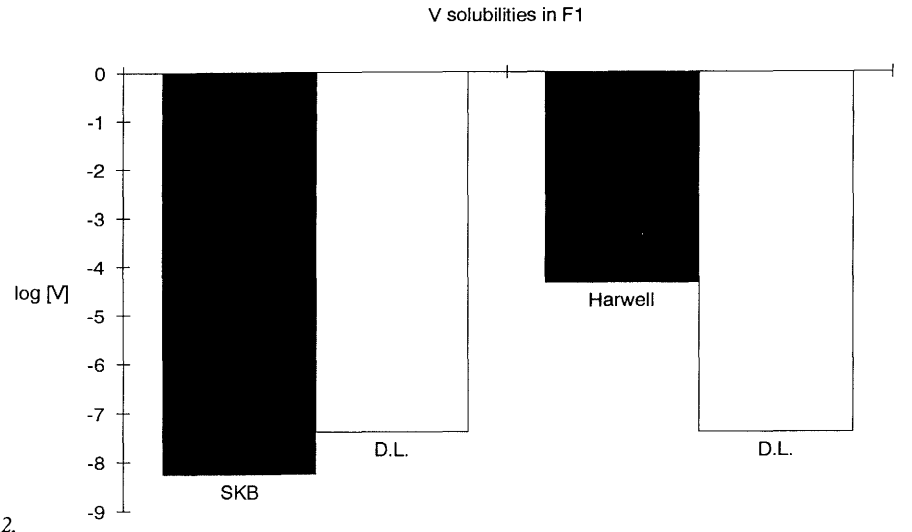

Figure 22.

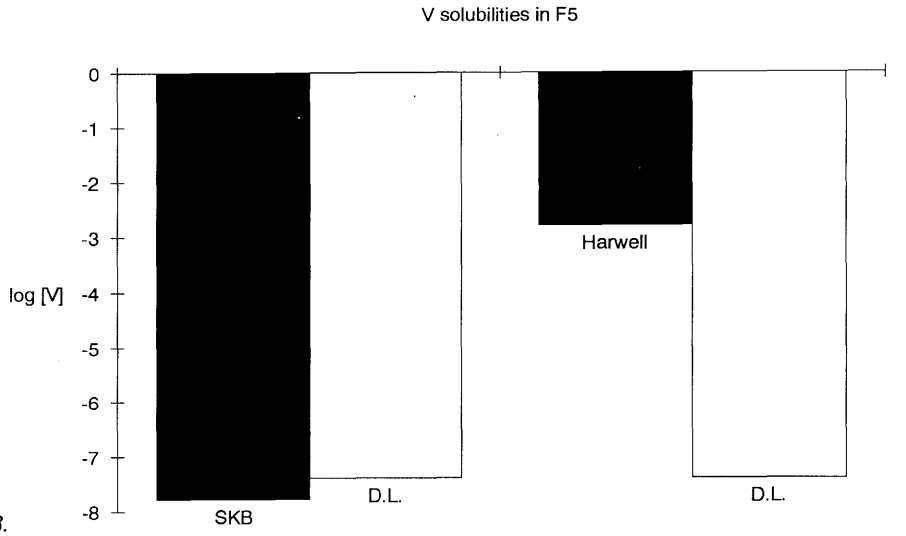

Figure 23.

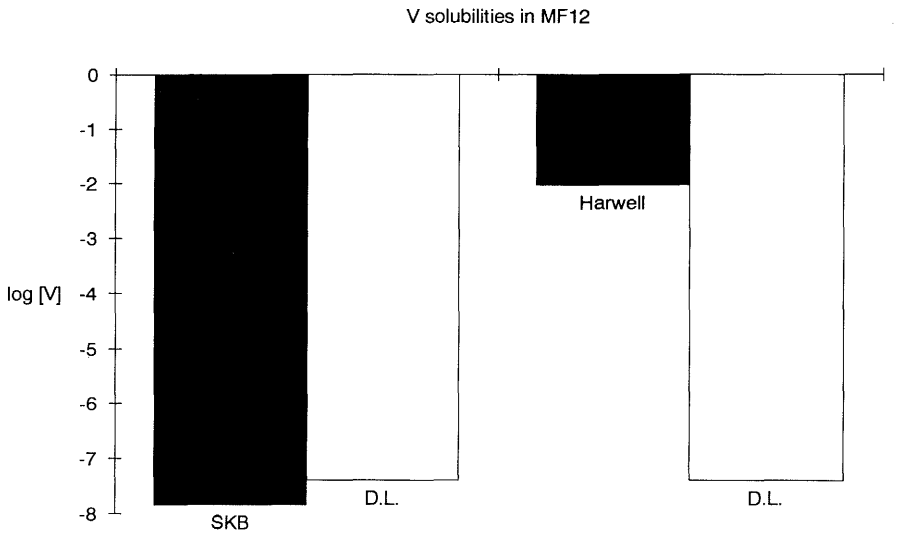

Figure 24.

Figures 22 – 24. Calculated (black columns) versus measured (white columns) vanadium solubilites in the selected F1, F5 and MF12 groundwaters.

3.7. Aluminium

Aluminium can hardly be considered a trace element. The objective in calculating the Al(III) solubilities was to test whether the modellers could reproduce one of the important geochemical parameters which may be responsible (by weathering of K-feldspar) for buffering the pH at the redox front. The results of the solubility-limiting calculations are given in Tables XXI-XXIII and show good agreement between the different modellers. The calculated aluminium concentrations agree within 0.5 – 1 log units. Kaolinite is assumed to be the solubility-limiting phase which, in all cases, is in agreement with mineralogical information. The calculated Al concentrations agree quite well with those measured (see Figs. 25-27).

The aqueous speciation of Al in the F1, F5 and MF12 groundwaters is dominated by Al(III) fluoride complexes, although some Al(III) hydrolysis complexes are also formed. The results from the speciation column measurements are quite ambiguous in the case of Al. Both the cationic and anionic resins exchange with aluminium in approximately equal ratios. This would be consistent with the speciation proposed by KTH with 42% $Al(OH)_4^-$ and 50% $Al(OH)_2^+$, or the existence of cationic and anionic Al(III) fluoride complexes as proposed by Atkins. In general, ≥ 95% of the Al is in 'true solution' – the remnant probably being present as colloidal size aluminosilicates.

TABLE XXI
Results of the solubility calculations of aluminium in the F1 groundwater.

Modeller	[Al] mol dm^{-3}	Solubility-limiting phase	Aqueous (%) speciation
SKB	$4.1 \cdot 10^{-6}$	Kaolinite	AlF^{2+} (62) AlF_2^+ (26)
KTH	$1.58 \cdot 10^{-6}$	Kaolinite	$Al(OH)_3$ (19) $Al(OH)_2^{2+}$ (47)
Harwell	$8 \cdot 10^{-6}$	Kaolinite	AlF_2^+ (68) AlF^{2+} (24)
Atkins	$3 \cdot 10^{-6}$	Kaolinite	AlF_3 (13) AlF^{2+} (74) AlF_2^+ (12)

Kaolinite: $Al_2Si_2O_6(OH)_4$.

TABLE XXII

Results of the solubility calculations of aluminium in the F5 groundwater.

Modeller	[Al] mol dm^{-3}	Solubility-limiting phase	Aqueous (%) speciation
SKB	$6.3 \cdot 10^{-5}$	Kaolinite	AlF_3 (52) AlF_2^+ (45)
KTH	$1.35 \cdot 10^{-6}$	Kaolinite	AlF_3 (62) AlF_2^+ (27)
Harwell	$1 \cdot 10^{-5}$	Kaolinite	AlF_3 (74) AlF^{2+} (14)
Atkins	$7 \cdot 10^{-7}$	Kaolinite	AlF_3 (67) AlF_2^+ (19)

TABLE XXIII

Results of the solubility calculations of aluminium in the MF12 groundwater.

Modeller	[Al] mol dm^{-3}	Solubility-limiting phase	Aqueous (%) speciation
SKB	$3.0 \cdot 10^{-6}$	Kaolinite	AlF_3 (67) AlF_2^+ (28)
KTH	$6.91 \cdot 10^{-7}$	Kaolinite	AlF_3 (48) AlF_2^+ (30) $Al(OH)_3$ (15)
Harwell	$1 \cdot 10^{-5}$	Kaolinite	AlF_3 (74) AlF^{2+} (13)
Atkins	$1 \cdot 10^{-6}$	Kaolinite	AlF_3 (68) AlF_2^+ (18) AlF_4^- (14)

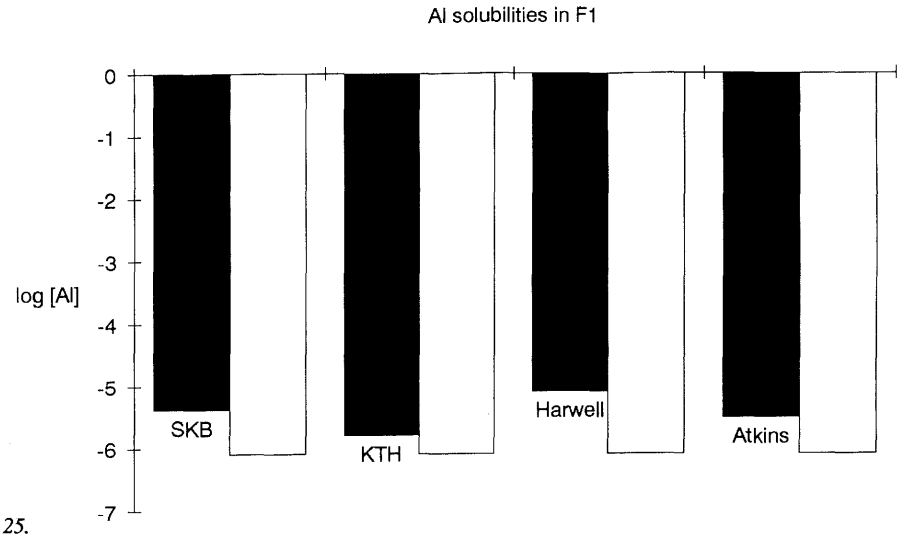

Figure 25.

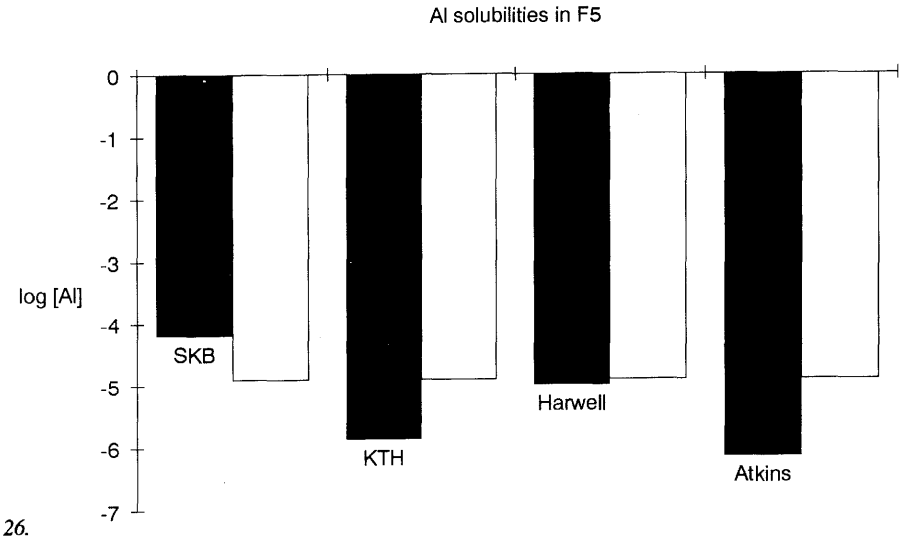

Figure 26.

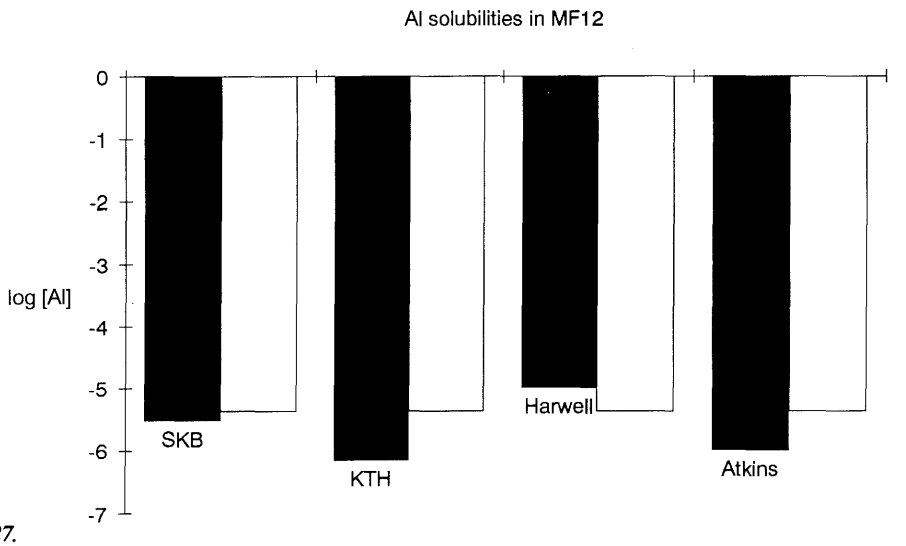

Figure 27.

Figures 25 – 27. Calculated (black columns) versus measured (white columns) aluminium solubilities in the selected F1, F5 and MF12 groundwaters.

3.8. Manganese

Manganese is another redox-sensitive element which is more mobile under reducing conditions than under oxidising ones. Manganese concentrations in natural waters are rarely controlled by the solubility of individual solid phases. The solubilities calculated by the modelling groups are quite high (see Tables XXIV-XXVI). The variations in the calculated concentrations are primarily the result of differences in the final pH values as the F1, F5 and MF12 groundwaters were equilibrated with rhodocrosite ($MnCO_3$). The measured Mn(II) concentrations are consistently much lower than the calculated solubilities (see Figs. 28-30). The correlation between Mn and iron in the parent rock indicates that the aqueous concentrations of manganese could be controlled by a Mn-Fe(III)-oxide solid solution (see Fig. 31). Mn is low in phonolites but relatively plentiful in syenites (~0.3%) at the Osamu Utsumi mine (Waber *et al.*, this report series; Rep. 2).

The aqueous speciation is dominated by the free ion Mn^{2+}. In the cases where the modellers allowed the pH to drift to values higher than 7, bicarbonate and carbonate complexes became the dominant ones. The results from the speciation column measurements show that Mn(II) is consistently associated with positively charged species. This is in agreement with the calculated speciation as Mn^{2+} or $MnHCO_3^+$. In general, >90% of the Mn is present in true solution and significant colloidal contents are found only in very organic-rich, near-surface water.

TABLE XXIV
Results of the solubility calculations of manganese in the F1 groundwater.

Modeller	[Mn] mol dm^{-3}	Solubility-limiting phase	Aqueous (%) speciation
SKB	High	$MnCO_3(s)$	Mn^{2+} (98)
KTH	3.77	$MnCO_3(s)$	Mn^{2+} (98)
Harwell	$3 \cdot 10^{-2}$	$MnCO_3(s)$	$MnHCO_3^+$ (99)
Atkins*	$2 \cdot 10^{-4}$	$MnCo_3(s)$	$MnCO_3(aq)$ (91)

(*) pH drift to 8.5 as a result of PHREEQE calculations.

TABLE XXV

Results of the solubility calculations of manganese in the F5 groundwater.

Modeller	[Mn] mol dm^{-3}	Solubility-limiting phase	Aqueous (%) speciation
SKB	0.1	$MnCO_3(s)$	Mn^{2+} (94)
KTH	$2.3 \cdot 10^{-2} \Rightarrow 1.2 \cdot 10^{-2}$	$MnCO_3(s)$	Mn^{2+} (98)
Harwell*	$2 \cdot 10^{-4}$	$MnCO_3(s)$	$MnHCO_3^+$ (93)
Atkins**	$2 \cdot 10^{-3}$	$MnCo_3(s)$	$MnCO_3(aq)$ (76) Mn^{2+} (20)

(*) pH drift to 6.9 as a result of HARPHRQ calculations.

(**) pH drift to 7.6 as a result of PHREEQE calculations.

TABLE XXVI

Results of the solubility calculations of manganese in the MF12 groundwater.

Modeller	[Mn] mol dm^{-3}	Solubility-limiting phase	Aqueous (%) speciation
SKB	$5 \cdot 10^{-2}$	$MnCO_3(s)$	Mn^{2+} (99)
KTH	0.14	$MnCO_3(s)$	Mn^{2+} (98)
Harwell*	$2 \cdot 10^{-4}$	$MnCO_3(s)$	Mn^{2+} (98)
Atkins**	$2 \cdot 10^{-3}$	$MnCO_3(s)$	$MnCO_3(aq)$ (89)

(*) pH drift to 7.0 as a result of HARPHRQ calculations.

(**) pH drift to 8.1 as a result of PHREEQE calculations.

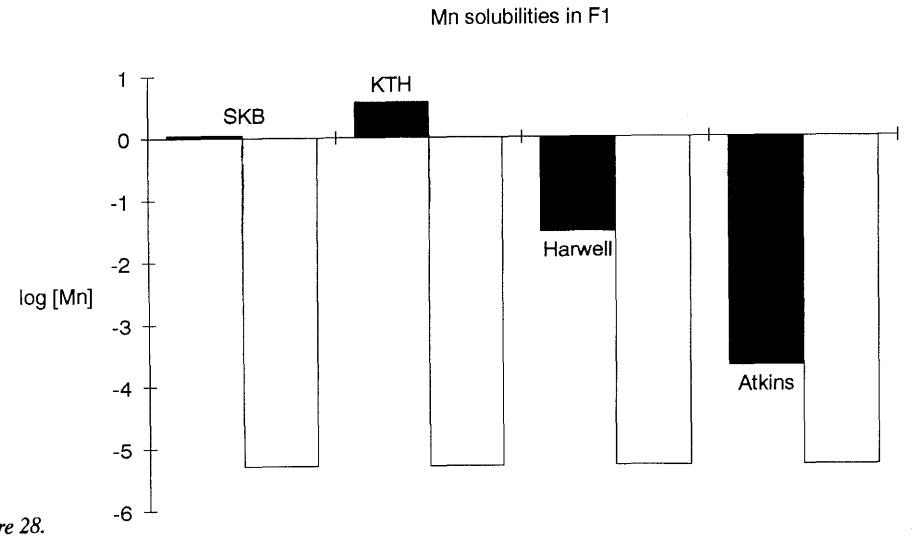

Figure 28.

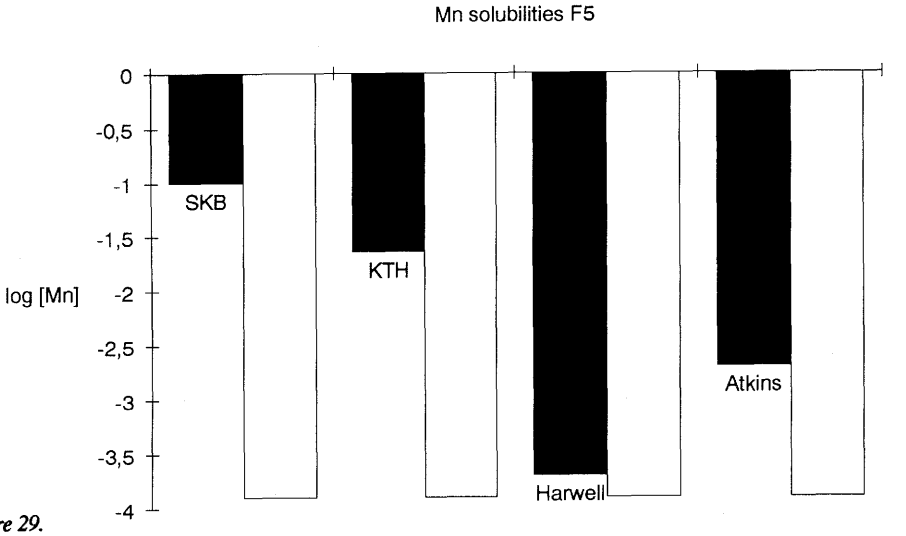

Figure 29.

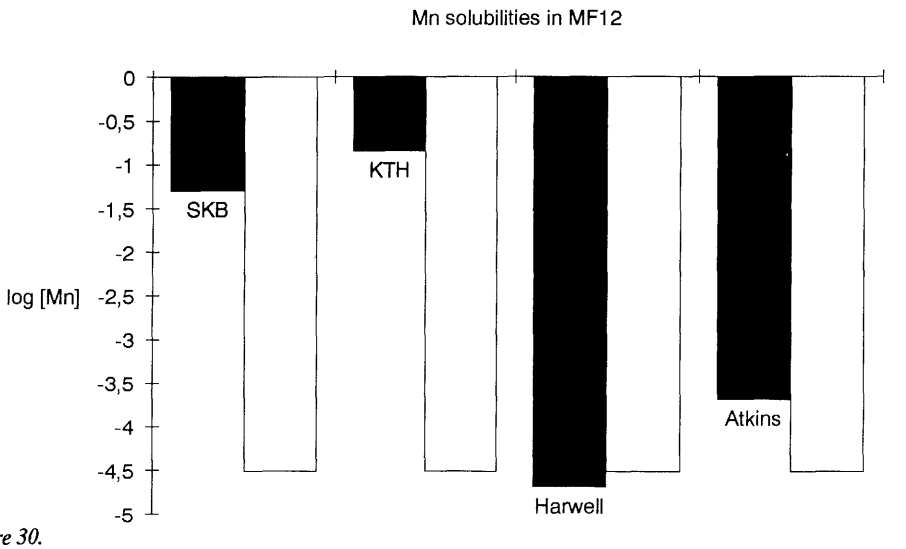

Figure 30.

Figures 28 – 30. Calculated (black columns) versus measured (white columns) manganese solubilites in the selected F1, F5 and MF12 groundwaters.

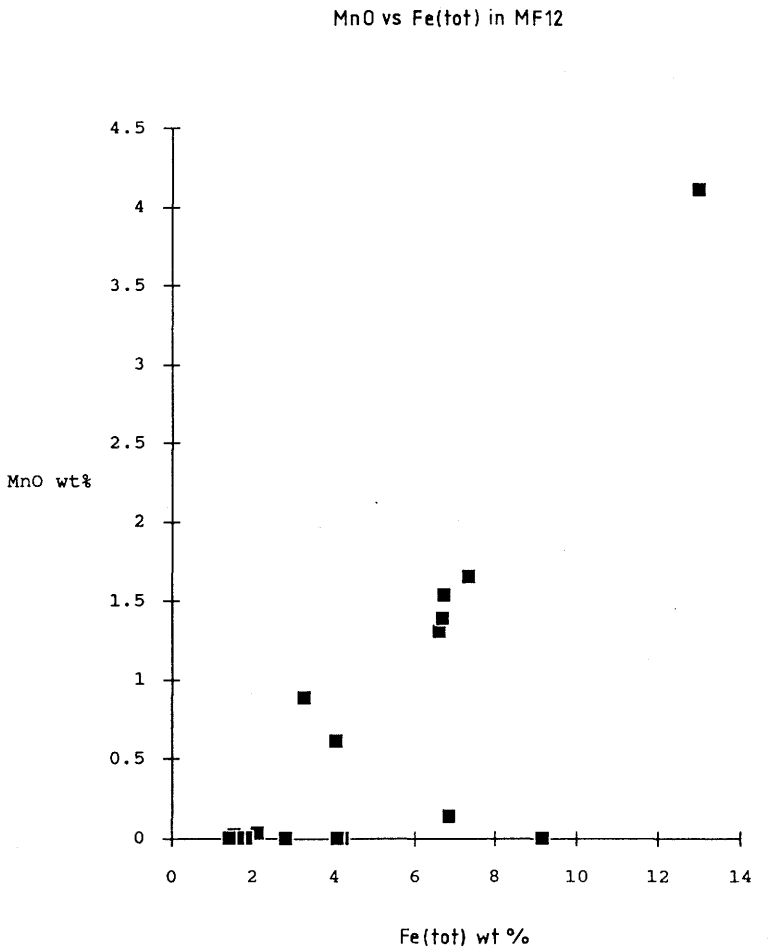

Figure 31. Manganese versus iron content in the MF12 host phonolite rock.

3.9. Zinc

The predicted solubilities in the F1, F5 and MF12 waters are given in Tables XXVII-XXIX respectively. The agreement between the three modelling groups is poor. SKB assumed equilibrium with $ZnFe_2O_4$, which resulted in very low Zn(II) concentrations. The KTH group assumed equilibrium with $ZnCO_3$, while the Harwell group chose $Zn_3(PO_4)_2(s)$ as the solubility-limiting phase. In these cases the predicted Zn(II) concentrations were quite high. The comparison with the measured values gives a similar picture to that of nickel (see Figs. 32-34), although it should be emphasised that the Zn concentrations are well above detection limits, thus illustrating the non-conservatism of the SKB predictions. In Figure 35 it is possible to see that Zn is also correlated to iron in the oxidised part of the MF12 parent rock.

The aqueous speciation is predicted to be dominated by the free ion Zn^{2+} in all cases. Zn is, however, generally $\geq 99\%$ in true solution, which indicates less correlation with Fe in colloids than was the case for Ni; in this respect Zn is more similar to Sr.

TABLE XXVII
Results of the solubility calculations of zinc in the F1 groundwater.

Modeller	[Zn] mol dm^{-3}	Solubility-limiting phase	Aqueous (%) speciation
SKB	$3\ 10^{-12}$	$ZnFe_2O_4$	Zn^{2+} (99)
KTH		$ZnCO_3(s)$	Zn^{2+} (98)
Harwell	$1.1\ 10^{-3}$	$Zn_3(PO_4)_2$	Zn^{2+} (96)

TABLE XXVIII
Results of the solubility calculations of zinc in the F5 groundwater.

Modeller	[Zn] mol dm^{-3}	Solubility-limiting phase	Aqueous (%) speciation
SKB	$8\ 10^{-11}$	$ZnFe_2O_4$	Zn^{2+} (93)
KTH		$ZnCO_3(s)$	Zn^{2+} (98)
Harwell	$5.7\ 10^{-5}$	$Zn_3(PO_4)_2$	Zn^{2+} (96)

TABLE XXIX
Results of the solubility calculations of zinc in the MF12 groundwater.

Modeller	[Zn] mol dm^{-3}	Solubility-limiting phase	Aqueous (%) speciation
SKB	$3\ 10^{-12}$	$ZnFe_2O_4$	Zn^{2+} (99)
KTH		$ZnCO_3(s)$	Zn^{2+} (98)
Harwell	$4.7\ 10^{-5}$	$Zn_3(PO_4)_2$	Zn^{2+} (98)

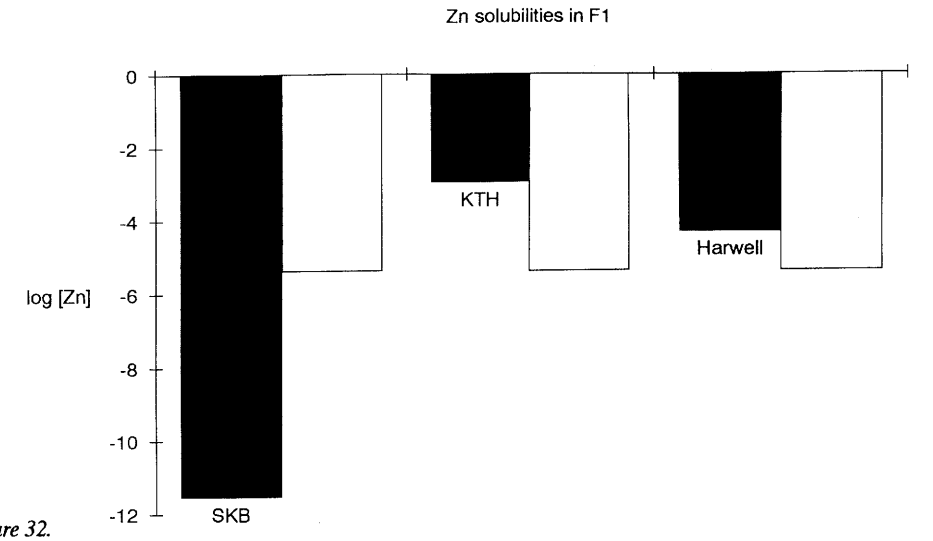

Figure 32.

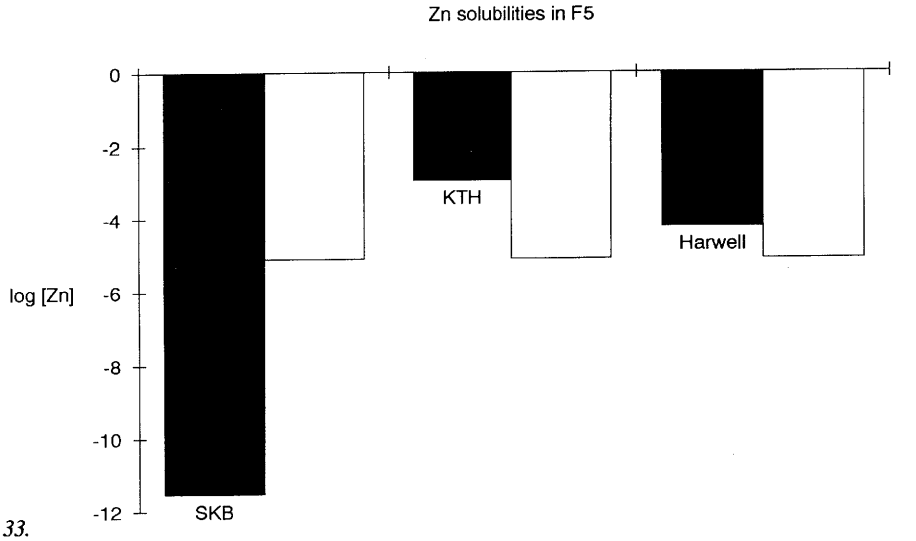

Figure 33.

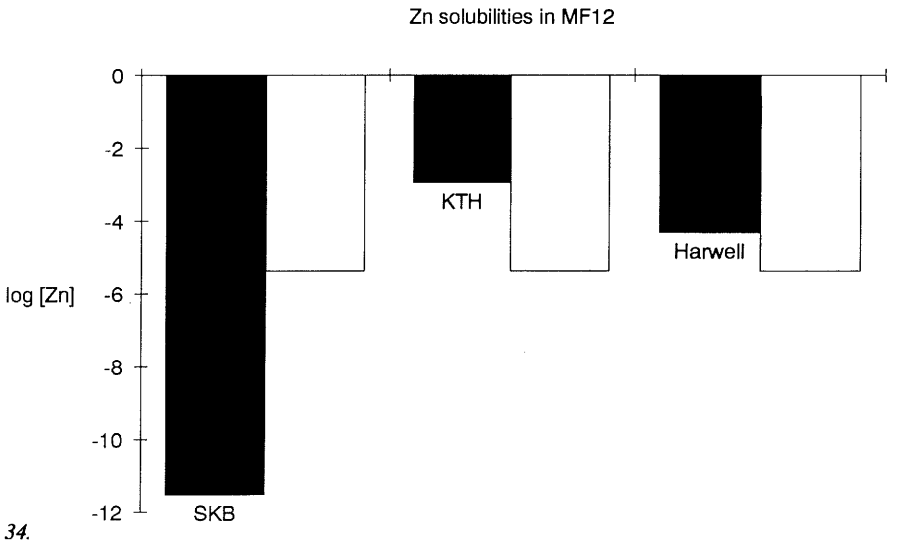

Figure 34.

Figures 32 – 34. Calculated (black columns) versus measured (white columns) zinc solubilites in the selected F1, F5 and MF12 groundwaters.

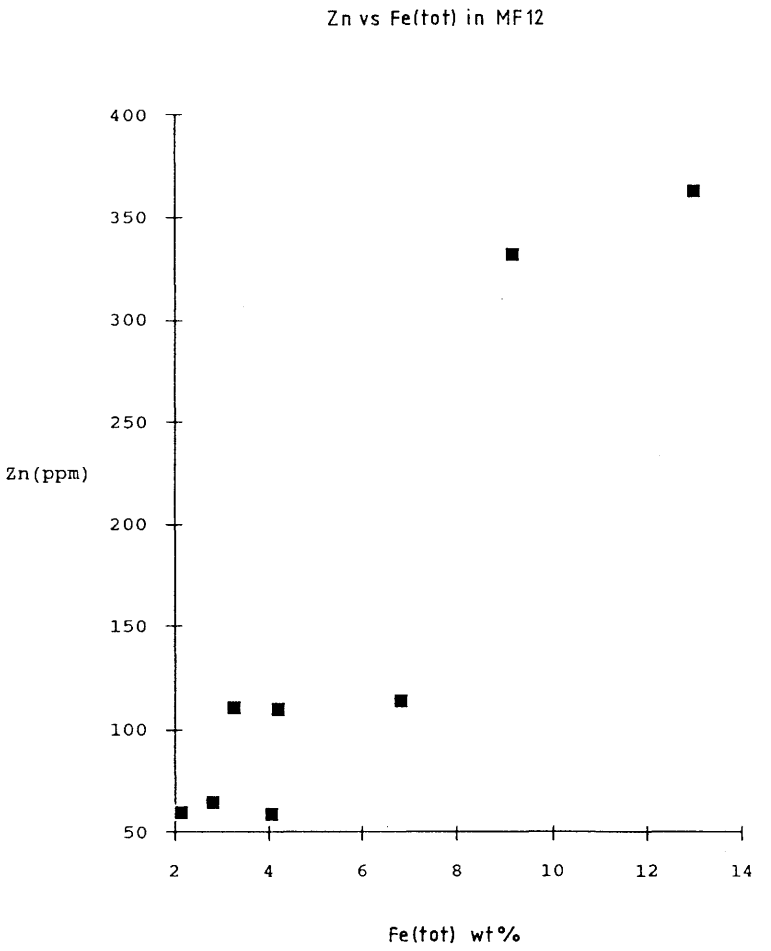

Figure 35. Zinc versus iron content in the oxidised MF12 host phonolite rock.

4. Summary, conclusions and recommendations

The Poços de Caldas project has provided an excellent opportunity for testing the thermodynamic models used in repository performance assessment. In general, the predictions of the various modelling groups were reasonably comparable and consistent with field observations. Only a few specific cases can be identified where model predictions of solubility were highly non-conservative and these involved only Ni and Zn when a ferrite mineral is taken as the solubility-limiting solid. It appears unlikely that such minerals are formed under low-temperature conditions and, unless there is evidence for their formation in a specific environment, it is strongly recommended that ferrite minerals be excluded in solubility limit calculations.

For the waters which are most likely to be saturated (F5 and MF12), agreement between predicted and observed concentrations is best for Th, Pb and Al. Overprediction of Th solubility occurs if phosphate complexes are included, but this could be due either to exaggeration of the phosphate concentration (measured values were at or below the detection limit) or overestimated stability constants for such complexes.

For all other elements, measured concentrations were below predicted solubility limits. For elements such as V this may reflect source-term limits but, for U and Sr in particular, specific minerals containing these elements are present along with evidence of their mobilisation. For Sr, the discrepancy probably simply reflects the absence of key minerals (e.g. goyazite) from the databases used. For U, the discrepancy could simply be due to uncertainties in the databases used (which were generally selected to "conservatively" overpredict solubility) or could, as in the case of Ni, Zn and Mn, reflect concentration limits set by coprecipitation with Fe oxyhydroxides which are formed at the redox front and could act as efficient scavenging agents for trace elements.

The role of coprecipitation or solid solution of radionuclides in Fe oxyhydroxides has not been quantitatively included in performance assessment models due to lack of appropriate data. This study strongly suggests that neglecting this phenomenon is 'conservative', but may overestimate concentrations by many orders of magnitude. This conclusion is in agreement with studies of uranium in marine sediments (Santschi *et al.*, 1988) and trace elements in redox halos (Hoffmann, 1990). In order to realistically model trace element concentrations in a region of Fe oxyhydroxide formation (e.g. in a corroding steel canister (NAGRA, 1985) or at a radiolytic redox front (KBS, 1983)), it is recommended that coprecipitation/solid solution models be developed.

The extent of agreement between predictions of speciation was very variable, being very good for some elements(e.g. Sr, Ni, Zn, Al, Mn) and rather poor for others (e.g. U,

Th). The discrepancies involved reflect both inherent differences in the complexity of the aqueous chemistry of these elements, but also variability in the extent of their databases. Of key significance from a safety assessment viewpoint is the charge of the predominant aqueous complex(es). For the pH range considered (5.0 – 7.0), the mineral surface charge is expected to be mainly positive. Hence, free cations or cationic complexes would be expected to sorb more than neutral complexes which, in turn, sorb much more than anionic complexes. In this study, speciation predictions could be tested, to some extent, against field ion-exchange separation results and colloid fractionation studies. It should be emphasised that the former technique is not yet well-established in this application, while information from the latter is rather indirect. Nevertheless, predicted speciation and ion-exchange/colloid fractionation results showed reasonable consistency for Al and Mn and, in some cases, U and Th. Given the great importance of sorption in the geosphere, it is recommended that techniques for in-situ speciation be further developed and applied to testing model predictions.

Finally, it should be noted that the Poços de Caldas project has accumulated a unique geochemical database for model testing. The modelling carried out within the Project has been limited by time and resources available, but opportunities exist for further tests, either within national programmes or international initiatives (e.g. CHEMVAL).

5. Acknowledgements

Without the active participation and interest of the different modelling groups, this study would not have been possible. Albert Losher helped in the compilation of the thermodynamic databases.

6. References

Baes, C.F. and Mesmer, R., 1976. The hydrolysis of cations. John Wiley and Sons, New York.

Baeyens, B. and McKinley, I.G., 1989. A PHREEQE database for Pd, Ni and Se. *NAGRA Tech. Rep.* (NTB 88-28), Baden, Switzerland.

Bruno, J. and Puigdomènech, I., 1989. Validation of the SKBU1 Uranium Thermodynamic Data Base for its use in Geochemical Calculations with EQ3/6. Scientific Basis for Nuclear Waste Management. XII. *Mat. Res. Soc. Symp. Proc.*, 127, 887-896.

Bruno, J., Sandino, A. and Folke, F., 1990. The solubility of $(UO_2)_3(PO_4)_2$ 4 H_2O in alkaline to neutral pH values. *Radiochim. Acta* (in press).

Hoffmann, B.A., 1990. Reduction spheroids from northern Switzerland: mineralogy, geochemistry and genetic models. *Chem. Geol.*, 81, 55-81.

KBS, 1983. KBS-3. SKBF/KBS, 5 Vols., Stockholm, Sweden.

Lindberg, R.D. and Runnells, D.D., 1984. Ground water redox reactions: An analysis of equilibrium state applied to Eh measurements and geochemical modelling. *Science*, 225, 925-927.

Santschi, P.H., Bajo, C., Mantovani, M., Orciuolo, D., Cranston, R.E. and Bruno, J., 1988. Uranium in pore waters from the North Atlantic (GME and Southern Nares Abyssal Plain sediments). *Nature* 331 (6152), 155-157.

Schweitzer, D.G., 1989. Inconsistencies in thermodynamic analysis of long-term isolation of high-level waste. *Nucl. Technol.*, 84, 88-92.

NAGRA, 1985. Projekt Gewähr (NGB 85-01 to -08; English Summary, NGB 85-09), Baden, Switzerland.

Appendix 1

Results of the first model intercomparison.

Appendix 1
Results of the first model intercomparison.

As explained in section 2, the main phase of model testing was preceded by a model intercomparison based on major element analyses of water samples from Morro do Ferro. The actual water samples used were GW-48, -49 and -50 from boreholes MF10, -11 and -12 respectively (Nordstrom *et al.*, this report series; Rep. 6). The results of this study are summarised in Tables 1-I to 1-III. In general, there was fair agreement between modellers and predicted solubilities were lower than observed concentrations.

Some points may be noted from these tables:

1) In all waters U(VI) predominates. U is fairly soluble ($\sim 10^{-6} - 10^{-7}$ M) with uncharged carbonato or phosphato complexes dominating aqueous speciation.

2) Th is, as expected, fairly insoluble (solubility set by ThO_2), but apparently this solubility may be increased due to phosphato complexation.

3) Pb is predicted to be fairly soluble in this system, present in solution as free Pb^{2+} or the uncharged carbonato complex.

4) V is predicted to be solubility-limited by a mixed U/V mineral (tyuyamunite) with an anionic hydroxo species predominating in solution.

5) Ni is modelled to be extremely insoluble with concentrations limited to $\sim 10^{-12}$ M by a ferrite solid phase.

6) In all waters Sn solubility is set by SnO_2 and an uncharged aqueous hydroxo species is predicted to predominate.

7) Se concentration is limited by elemental Se solubility to $\sim 10^{-6}$ M, with selenite as the main species in the aqueous phase.

8) Ra is fairly soluble ($\sim 10^{-6}$ M) with the free ion predominating in solution and the sulphate being the limiting solid phase.

TABLE 1-I

Results MF10 (GW-48): pH = 6.9, Eh = 100 mV

Element	Solubility-limiting phase	Total concentration (mol dm^{-3})	Predominant species
U	$UO_2(OH)_2xH_2O(s)$	$3.7x10^{-7}$* $3.4x10^{-9}$**	UO_2CO_3 (aq)
Th	$ThO_2(s)$	$3.5x10^{-10}$* $2.6x10^{-10}$**	$Th(OH)_4$ (aq)
Pb	$PbCO_3(s)$	$5x10^{-4}$* $<2x10^{-7}$**	$PbCO_3$, Pb^{2+}
V	Tyuyamunite[1)]	$1.4x10^{-7}$* $<3.9x10^{-6}$**	$VO_2(OH)_2^-$
Ni	$NiFe_2O_4$	$8.4x10^{-13}$* $<5.1x10^{-6}$**	Ni^{2+}
Sn	SnO_2	$2.2x10^{-8}$*	$Sn(OH)_4$
Se	Se(black)	$1.8x10^{-6}$*	$HSeO_3^-$
Ra	$RaSO_4(s)$	$5x10^{-6}$*	Ra^{2+}

* calculated

** measured

1) $Ca(UO_2)_2(VO_4)_2$.

TABLE 1-II
Results MF11 (GW-49): pH = 5.6, Eh = 200 mV

Element	Solubility-limiting phase	Total concentration (mol dm^{-3})	Predominant species
U	$(UO_2)_3(PO_4)2(s)$	$1x10^{-6*}$ $5.4x10^{-9**}$	UO_2HPO_4 (aq)
Th	$ThO_2(s)$	$9.6x10^{-8*}$ $8.5x10^{-10**}$	$Th(HPO_4)_2$ (aq)
Pb	$PbCO_3(s)$	$5.3x10^{-4*}$ $< 2.4x10^{-7**}$	Pb^{2+}
V	Tyuyamunite	$1.4x10^{-7*}$ $< 3.9x10^{-6**}$	$VO_2(OH)_2^-$
Ni	$NiFe_2O_4$	1.10^{-12*} $< 1.4x10^{-6**}$	Ni^{2+}
Sn	SnO_2	$2.2x10^{-8*}$	$Sn(OH)_4$ (aq)
Se	Se(black)	$1.8x10^{-6*}$	$HSeO_3^-$
Ra	$RaSO_4(s)$	$6.9x10^{-6*}$	Ra^{2+}

* calculated
** measured

TABLE 1-III
Results MF12 (GW-50): pH = 6.0, Eh = 240 mV

Element	Solubility-limiting phase	Total concentration (mol dm^{-3})	Predominant species
U	$(UO_2)_3(PO_4)2(s)$	$1.2x10^{-6*}$ $3.2x10^{-9**}$	UO_2CO_3 (aq) UO_2HPO_4 (aq)
Th	$ThO_2(s)$	$2.9x10^{-9*}$ 3.10^{-10**}	$Th(HPO_4)_3^{2-}$ (aq)
Pb	$PbCO_3(s)$	$5.3x10^{-4*}$ $< 2.4x10^{-7**}$	$PbCO_3^{(aq)}$
V	Tyuyamunite	$5.4x10^{-9*}$ $< 4x10^{-6**}$	$VO_2(OH)_2^-$
Ni	$NiFe_2O_4(s)$	$3.5x10^{-12*}$ $< 1x10^{-6**}$	Ni^{2+}
Sn	SnO_2 (s)	$2.2x10^{-8*}$	$Sn(OH)_4$ (aq)
Se	Se(black)	$1.8x10^{-6*}$	$HSeO_3^-$
Ra	$RaSO_4(s)$	$3.4x10^{-7*}$ $10^{-12} - 10^{-14**}$	Ra^{2+}

* calculated
** measured

Appendix 2

Comparison of thermodynamic databases.

TABLE 2-I
Inorganic aqueous species.

SPECIES	HARWELL	CHEMVAL	Livermore	SKBU1
$UL_3(CO_3)_6^{-6}$	+25.8	+26.05	25.76	26.20
$UL_2(OH)_3CO_3^-$	-	-19.434	-	-
$UL_3(OH)_3CO_3^+$	-24.9	-26.651	-24.85	-24.43
$ULHPO_4$	+11.0	+11.53(+11.39)	-	?
$UL(HPO_4)_2^{-2}$	+34.5	+34.33 (+33.86)	-	-
$ULH_2PO_4^+$	+13.4	+13.35 (+13.79)	33.59	?
$UL(H_2PO_4)_2$	+35.4	+35.343 (+36.03)	75.17	?
$UL(H_2PO_4)_3^-$	+56.7	+56.593 (+57.4)	-	?
$ULSO_4$	-6.3	-6.26	-6.45	-5.85
$UL(SO_4)_2^{-2}$	-4.9	-5.29	-4.94	-4.43
ULF^+	-4.3	-4.22	-4.12	-3.97
ULF_2	-0.6	-0.44	-0.36	-0.38
ULF_3^-	+2.0	+2.0	2.05	+1.9
ULF_4^{-2}	+3.2	+3.21	3.24	2.7
$ULCl^+$	-9.3	-8.74	-8.96	-8.83
$ULCl_2$	-9.9	-9.94	-	-10.1
$ULCl_3^-$	-11.6	-11.64	-	?
$ULH_3SiO_4^+$	-11.6	-10.96	-11.59	?
$ULNO_3^+$	-9.1	-	-	-9.26

TABLE 2-I (contd.).

SPECIES	HARWELL	CHEMVAL	Livermore	SKBU1
U(VI)				
$UL = UO_2^{+2}$	-9.2	-9.217	-9.2	-9.07
$ULOH^+$	-14.5	14.45	-14.45	-14.31
$UL(OH)_2$	-21.1	-21.22	-21.26	-21.12
$UL(OH)_3^-$	-99*	-33.00	-29.15	-29.04?
$UL(OH)_4^{-2}$	-45.6	-47.017	-41.00	-40.84
UL_2OH^{+3}	-21.1	-22.51	-21.2	-20.93
$UL_2(OH)_2^{+2}$	-24.1	-24.06	-24.06	-23.78
$UL_3(OH)_4^{+2}$	-39.6	-39.43	-39.6	-39.18
$UL_3(OH)_5^+$	-43.2	-43.31	-43.27	-42.84
$UL_3(OH)_7^-$	-62.9	-58.651	-60.06	-58.91
$UL_4(OH)_7^+$	-58.7	-58.56	-58.74	-58.17
$ULCO_3$	+0.3	+0.16	+0.31	+0.45
$UL(CO_3)_2^{-2}$	+7.4	+7.22	+7.43	+7.58
$UL(CO_3)_3^{-4}$	+12.1	+12.24	+12.14	+12.30

TABLE 2-I (contd.).

SPECIES	HARWELL	CHEMVAL	Livermore
Th			
$Th(OH)^{+3}$	-3.2	-2.34	-3.22
$Th(OH_2)^{+2}$	-6.9	-6.36	-6.96
$Th(OH_3)^{+}$	-11.7	-11.7	-11.72
$Th(OH)_4$	-15.9	-15.9	-15.92
$Th_2(OH)_2^{+6}$	-6.1	-5.41	-6.15
$Th_2(OH)_3^{+5}$	-	-8.44	-
$Th_4(OH)_8^{+8}$	-21.1	-20.08	-21.17
$Th_6(OH)_{14}^{+10}$	-	-38.83	-
$Th_6(OH)_{15}^{+9}$	-	-43.84	-36.85
$Th(CO_3)^{+2}$	+11.03	+11.03	-
$Th(HPO_4)^{+2}$	+23.2	+25.25 (+25.29)	-
$Th(HPO_4)_2$	+47.50	+47.49 (+50.72)	-
$Th(HPO_4)_3^{-4}$	+68.3	+68.3 (71.55)	-

TABLE 2-I (contd.).

SPECIES	HARWELL	CHEMVAL	Livermore
$Th(H_2PO_4)^{+3}$	+24.2	+24.07(24.82)	24.17
$Th(H_2PO_4)_2^{+2}$	+48.0	+47.98(+48.92)	47.97
$Th(H_3PO_4)^{+4}$	+23.6	+23.6(+23.73)	23.58
$ThSO_4^{+2}$	+5.5	+5.45(+5.86)	5.47
$Th(SO_4)_2$	+9.7	+9.73(+8.69)	9.73
$Th(SO_4)_3^{-2}$	+10.5	+10.5	10.52
$Th(SO_4)_4^{-4}$	+8.5	+8.48	8.50
ThF^{+3}	-	+8.44	8.06
ThF_2^{+2}	-	+15.06	14.29
ThF_3^{+}	-	+19.81	18.95
ThF_4	+22.3	+23.17	22.36
$ThCl^{+3}$	+1.38	+1.18	1.12
$ThCl_2^{+2}$	-1.10	+0.92	0.84
$ThCl_3^{+}$	-0.83	+1.71	1.66
$ThCl_4$	-1.74	+0.94	1.23
$ThNO_3^{+3}$	+1.6	-	-
$Th(NO_3)_2^{+2}$	+2.8	-	-
$Th(NO_3)_3^{+}$	+2.0	-	-
$Th(NO_3)_4$	+1.0-	-	-

TABLE 2-I (contd.).

SPECIES	HARWELL	CHEMVAL	Livermore
Mn(II)			
$Mn(OH)^{+}$	-10.59	-10.59 (-10.19)	-10.6
$Mn(OH)_3^{-}$	-34.8	-34.18 (-34.8)	-34.21
$Mn(OH)_4^{-2}$	-	-4.83	-48.29
$Mn_2(OH)^{+3}$	-	-10.6 (-10.14)	-10.56
$Mn_2(OH)_3^{+}$	-	-23.9 (-24.93)	-23.90
$MnCO_3$	-	+6.5	3.52
$MnHCO_3^{+}$	+11.6	+11.6 (+11.23)	11.62
$MnSO_4$	+2.26	+2.86	2.29
$Mn(NO_3)_2$	+0.60	-	0.60
MnF^{+}	+0.85	+0.85	1.35
$MnCl^{+}$	+6.1	+0.607 (+0.610)	-0.20
$MnCl_2$	+0.04	+0.041 (+0.25)	0.25
$MnCl_3^{-}$	-0.31	-0.305 (-0.310)	-0.32
$Mn(HPO_4)$	-	+16.09 (+16.32)	15.90
$Mn(HPO_4)_2^{-2}$	-	+29.52 (+29.97)	-

TABLE 2-I (contd.).

SPECIES	HARWELL	CHEMVAL	Livermore
Sr			
$SrOH^+$	-13.19	-13.2	-13.28
$Sr(OH)_2$	-28.51	-28.51	-
$SrCO_3$	+2.81	+2.85 (+2.35)	2.80
$SrHCO_3^+$	-	+11.59 (+11.57)	11.53
$SrSO_4$	+2.55	+2.55 (+2.48)	2.31
SrF_2	+0.50	+1.7 (+0.65)	0.76
SrF^+		+2.02	-
$SrCl^+$	+0.19	+0.20 (+0.33)	-
$SrCl_2$	0.00	-	-
$SrNO_3^+$	+0.82	-	0.81
$SrPO_4^-$	+4.18	+5.5 (+5.48)	5.51
$SrHPO_4$	-	+14.5 (+14.14)	14.89
$Sr(H_2PO_4)^+$	-	+20.30 (+20.28)	20.30

Appendix 3

The use of portable speciation equipment in groundwater studies at the Poços de Caldas field-site (Brazil).

Appendix 3

The use of portable speciation equipment in groundwater studies at the Poços de Caldas field-site (Brazil).

B.P. VICKERS

British Geological Survey, Keyworth, Nottingham NG12 5GG, (U.K.).*

1. Introduction

Various workers (eg. Miles *et al.*, 1983; Tuschall *et al.*, 1985 and Mantoura and Riley, 1975) have suggested the use of ion-exchange resins to speciate organo-metallic complexes in groundwater. During the development of a speciation scheme in these laboratories it was attempted to avoid changes in groundwater chemistry and interactions between various colloidal phases and ions in solution. Groundwater is passed, on-site, through a sequence of resins to remove organic, cationic and anionic species respectively. Trials were therefore carried out using resins which did not require the groundwater to be pre-treated, so maintaining the natural equilibria, pH and ionic strength of the water sample.

Portable equipment, involving the passage of water samples sequentially through a series of columns, was developed and is described by Breward and Peachey (1988). The recent availability of pre-packed columns covering a variety of newly-developed resins has led to redesigning of the equipment.

The value of the speciation equipment was recognised within the Poços de Caldas Project and a trip to the Osamu Utsumi mine and Morro do Ferro analogue sites was subsequently arranged for the end of November 1988.

2. Selection of columns for the speciation equipment

Between the initial development of the equipment and this trip, several problems with the original columns became apparent. It was thought that some organic matter and/or organo-metallic complexes were not retained by DEAE-cellulose (an anionic resin) and were not capable of absorbing U(V). Moreover, the resin often compacted in the column, thereby severely limiting the flow of water. All of the columns and fittings therefore had to be prepared by hand.

---

* B.G.S. Technical Report WI/89/9

However, new material (including new forms of DEAE-cellulose) in packed columns has recently become commercially available. Field and laboratory trials were carried out using these (Smith *et al.*, 1989), concentrating on an improved DEAE-cellulose column since it has been shown at Broubster, Scotland that the majority of organo-metallic complexes of uranium and thorium were retained by this type of resin. Although not all of the results from these trials had been fully assessed, the following packed columns were used at the Poços de Caldas field sites:

1. Waters "Accell" QMA, a strong anionic resin.
2. Waters "Accell" CM, a medium cationic resin.
3. Waters C_{18}, a resin retaining non-polar organic species.

The QMA column should remove most organic species, plus some inorganic anionic species and the CM should remove cationic species such as iron. The C_{18} column was added in an attempt to extract the organic species not retained by the QMA column.

It was decided to pass portions of water through each column separately, rather than sequentially as in the original design, to elucidate what each column was retaining. The equipment has capacity for four columns and the fourth place was usually taken by another QMA column (see Table 3-I) as a check on the reproducibility of the results.

Visual inspection of the CM column showed, for some samples, a great deal of red-brown coloration, thought to be due to iron hydroxides. A further CM column was added in-line for these samples (see Table 3-I).

TABLE 3-I
Samples collected and columns used in the study.

Borehole	Column			
	1	2	3	4
F1 (9-1WC11)	QMA	CM	C_{18}	QMA
F2 (9-1VC24)	QMA	CM	C_{18}	QMA
F3 (9-1NH47)	QMA	CM	C_{18}	QMA
F4 (8-1UK11)	QMA	CM(2)	QMA	CM(2)
F5 (MI-55a)	QMA	CM(2)	C_{18}	QMA
F5 (MI-55b)	QMA	CM(3)	C_{18}	CM(3)
SW03	QMA	CM	C_{18}	QMA
MF10	QMA	CM	C_{18}	QMA
MF12	QMA	CM	C_{18}	QMA

Figures in brackets indicate how many columns were used.

3. Collection of samples

Boreholes F1, F2, F3, F4, F5 (mine locations 9-1WC11, 9-1VC24, 9-1NH47, 8-1UK11 and MI-55 respectively) and SW03 were sampled from the Osamu Utsumi uranium mine site and boreholes MF10 and MF12 were sampled from the Morro do Ferro site. The Eh measurement at borehole F5 suggested that the hole had not been pumped properly, so a fresh sample (MI55b) was taken after it had been pumped to obtain a steady Eh value. Water was pumped from each borehole and immediately filtered through a 0.45 μm Millipore membrane. Portions of filtered water were taken by local staff for analysis at the Nuclebras laboratories and between 3 and 5 litres of water were collected for the speciation experiments. Most samples were passed through the speciation equipment directly on-site to avoid the many problems associated with the storage and transportation of samples. However, due to lack of field time, some samples (MI55a, MI55b, MF10 and MF12) were collected and passed through the equipment in a field laboratory later the same evening.

Five hundred ml of water was passed through each column and, for practical reasons, this was split into two portions of 250 ml. As the equipment had not been fully evaluated, a separate 500 ml portion of water was passed through each column individually rather than sequentially as in the original design. One hundred ml of deionised water was then passed through each of the columns to wash out any remaining sample solution. The columns were kept in a refrigerator when not in use.

At the same time as the first 250 ml portion of water was taken, 45 ml of water was also taken and acidified with 5 ml of concentrated nitric acid to be analysed for metals by Inductively Coupled Plasma Atomic Emission Spectrometry (ICP-AES) and Inductively Coupled Plasma Mass Spectrometry (ICP-MS) at BGS. A further 20 ml portion was also taken to be analysed for organic matter by Ultra-violet spectroscopy (UV), with a further 20 ml portion being collected for UV after the water had passed through a particular column.

4. Analysis by Ultra-violet spectroscopy

Ultra-violet spectroscopy can be used to give a rapid indication of the presence of organic material in water samples. In the BGS laboratories it has been found preferable to measure samples at 254 nm, thus minimising interference from inorganic ions such as iron.

Samples were taken prior to passing the water sample through the columns and after the sample had passed through each column to give an indication of the amount of UV-absorbable organic matter retained by each column.

Unfortunately, it was not possible to take measurements until the end of the trip, by which time it was noted that many samples contained a red-brown precipitate, presumably iron hydroxides. Duplicate measurements did not always agree well and for some samples the measurements taken after the sample had passed through a column were higher than those taken before the sample had passed through. This was thought to be due to interference by colloidal iron hydroxides. This section of the work was therefore not pursued or the results reported.

5. Elution of the columns

The columns were eluted using the following procedures:

5.1. QMA

a) NaOH. Eluted with 10 ml of 0.5N NaOH, the eluate transferred to a 25 ml volumetric flask and made up to volume with distilled water. 5 ml of concentrated HNO_3 was then added.

b) HCl. After the column had been washed with distilled water, the column was eluted with 10 ml of 0.5N HCl. The eluate was transferred to a 25 ml volumetric flask and made up to volume with distilled water.

5.2. CM

Eluted with 10 ml of 0.5N HCl, the eluate transferred to a 25 ml volumetric flask and made up to volume with distilled water.

5.3. C_{18}

a) CH_3OH. Eluted with 10 ml of CH_3OH, which was then "blown off" under N_2. The residue was taken up in 5 ml of 0.5N HCl and 2.5 ml of CH_3OH, transferred to a 25 ml volumetric flask and made up to volume with distilled water.

b) HCl. After the column had been washed with distilled water, the column was eluted with 10 ml of 0.5N HCl. The eluate was transferred to a 25 ml volumetric flask and made up to volume with distilled water.

The stationary phases of the columns are bonded to a silica surface on which residual silanol (SiOH) groups are present. These groups result in secondary cationic interactions, so the QMA and C_{18} columns were eluted with HCl to remove any complexes exchanged onto these sites. Secondary iron oxides had also been found to be retained by the DEAE-cellulose column used originally.

Due to insufficient analytical time only a few of the columns in position 4 were eluted.

6. Analysis of the eluates

The eluted sample solutions were initially analysed for a range of elements (Ca, Mg, Na, K, P, S, Si, Ba, Sr, Mn, Fe, Al, Co, Ni and U) by ICP-AES. Uranium, if below the detection limit of the ICP-AES, and thorium were then determined by ICP-MS. Samples high in uranium were diluted prior to thorium being determined as such samples can contaminate the more sensitive ICP-MS causing "memory effects".

The small amount of CH_3OH present in the eluates from the C_{18} columns was sufficient to cause interferences with the analyses. The solutions were diluted to minimise the effects of the CH_3OH, but this increased the detection for some of the results. These diluted solutions were only analysed for uranium and thorium by ICP-MS.

7. Results and discussion

The results for the levels found in each eluate are shown in Table 3-II. As well as uranium and thorium, results for iron, aluminium and manganese are shown, these elements being commonly associated with groundwater colloidal matter. At all of the Osamu Utsumi mine boreholes, at least 90% of the uranium is retained on the CM columns (see Figure 3-1), indicating an association with cationic species. However, at sites F1, F2, F4 and F5 a significant percentage of uranium is also found in the NaOH eluate of the QMA column, suggesting association with anionic organic species. Very little uranium is found associated with the C_{18} column. Some of the thorium levels are too low for any conclusions to be drawn, but in boreholes F2, F3, F5 (MI-55b) and SW03

TABLE 3-II

Results showing the level of metals eluted from each column using various reagents.

	U		Th	Fe	Al	Mn
	µg	ng	ng	ng	µg	µg
Borehole F1 (9-1WC11)						
Amount passed through		2500	30	750	125	74
Amount recovered:						
QMA – NaOH		1020	< 0.3	1	4	< 0.12
– HCl		1700	7.5	15	16	< 0.10
CM	1.75	2375	1.25	37	10	75
C_{18} – CH_3OH		450	< 125	nd	nd	nd
– HCl		2.5	< 0.25	3	5	< 0.10
Borehole F2 (9-1VC24)						
Amount passed through		2500	10	810	25	119
Amount recovered:						
QMA – NaOH	2.4	1500	< 0.3	3	16	< 0.12
– HCl		1075	5	39	99	< 0.10
CM	1.75	2450	< 0.25	84	69	114
C_{18} – CH_3OH		< 125	< 125	nd	nd	nd
– HCl		15	< 0.25	13	31	< 0.10
Borehole F3 (9-1NH47)						
Amount passed through		1000	150	40,800	2470	8900
Amount recovered:						
QMA – NaOH		120	< 0.3	4	5	< 0.12
– HCl		150	50	60	48	< 0.10
CM – a		1150	80	305	275	103
– b		725	21.3	343	222	138
C_{18} – CH_3OH		< 125	< 125	nd	nd	nd
– HCl		5	12.5	14	20	< 0.10
Borehole F4 (8-1UK11)						
Amount passed through		27.500	150	1470	895	1455
Amount recovered:						
QMA – NaOH	13.8	13,380	< 0.3	2	29	< 0.12
– HCl	6.5	7300	< 0.25	27	116	0.15
CM	26.3	nd	< 5	97	137	503

TABLE 3-II (contd.)

	U		Th	Fe	Al	Mn
	μg	ng	ng	ng	μg	μg
Borehole F5 (MI-55a)						
Amount passed through		7000	< 5	6000	480	1750
Amount recovered:						
QMA – NaOH		1930	< 0.3	16	43	< 0.12
– HCl	1.5	2800	< 0.25	184	126	0.15
CM	3	8225	20	1470	88	180
C_{18} – CH_3OH		215	< 125	nd	nd	nd
– HCl		650	5	216	63	< 0.10
Borehole F5 (MI-55b)						
Amount passed through		9000	50	5850	710	1600
Amount recovered:						
QMA – NaOH	2.7	4290	< 0.3	20	89	< 0.12
– HCl	3.5	4450	< 0.25	263	175	0.33
CM – a		10,000	10	1575	107	156
– b		12.5	1.5	605	71	281
– c		15	1.25	213	44	525
C_{18} – CH_3OH		243	< 125	nd	nd	nd
– HCl		400	12.5	148	102	< 0.10
Borehole SW03						
Amount passed through	2070	–	22,000	3110	4400	3875
Amount recovered:						
QMA – NaOH	4.2	3480	< 0.3	0.8	< 1.5	< 0.12
– HCl	5.5	6825	50	11	6	< 0.10
CM	1960	nd	23,000	19	290	2
C_{18} – CH_3OH		< 125	< 125	nd	nd	nd
– HCl		12.5	7.5	1	< 1.2	< 0.10
Borehole MF10						
Amount passed through		1000	40	610	140	1620
Amount recovered:						
QMA – NaOH		810	< 0.3	0.7	< 1.5	< 0.12
– HCl		75	7.5	27	7	0.13
CM		1075	5	42	< 1.2	167
C_{18} – CH_3OH		550	< 125	nd	nd	nd
– HCl		10	0.25	8	3	< 0.10

TABLE 3-II (contd.)

	U		Th	Fe	Al	Mn
	µg	ng	ng	ng	µg	µg
Borehole MF12						
Amount passed through		1000	50	510	475	540
Amount recovered:						
QMA – NaOH		690	< 0.3	10	30	< 0.12
– HCl		400	12.5	260	91	0.45
CM		925	1.25	46	36	473
C_{18} – CH_3OH		80	< 125	nd	nd	nd
– HCl		12.5	0.5	20	45	< 0.10

nd = not determined
Results are quoted as total ng or µg not µg/ml.

Detection limits:
U (ICP-AES) = 50 ppb
U (ICP-MS) = 0.05 ppb
Th (ICP-MS) = 50 ppb
Fe (ICP-AES) = 0.02 ppm
Al (ICP-AES) = 0.05 ppm
Mn (ICP-AES) = 0.004 ppm

thorium is mainly associated with cationic species. Previous work carried out at the site found low levels of DOC and high levels of iron, leading to the suggestion that colloidal iron-oxyhydrates were the main carriers of uranium, thorium and rare-earth elements. The work described here lends support to this theory. However, the overall charge on colloidal material can be affected by pH and the nature of the attached ligands (James and Parks, 1982). It is possible that complex colloids could consist of both positively and negatively charged groups which could stick to either an anionic or cationic resin. Despite the low levels of DOC, a study of Figure 3-2 suggests that there is some sorption of uranium onto organic matter in those samples from the Osamu Utsumi mine site. There is no obvious relationship between thorium and DOC.

In the samples from Morro do Ferro, uranium is retained by all three columns (see Figure 3-1) and it is not possible to draw any positive conclusion as to its preferred ionic species. Although a small amount of thorium is present, the very low levels retained by the columns are too small to draw any definite conclusions. Although these samples have a higher level of DOC than those from the Osamu Utsumi mine, they do not show an increase in levels of uranium and thorium (see Figure 3-2).

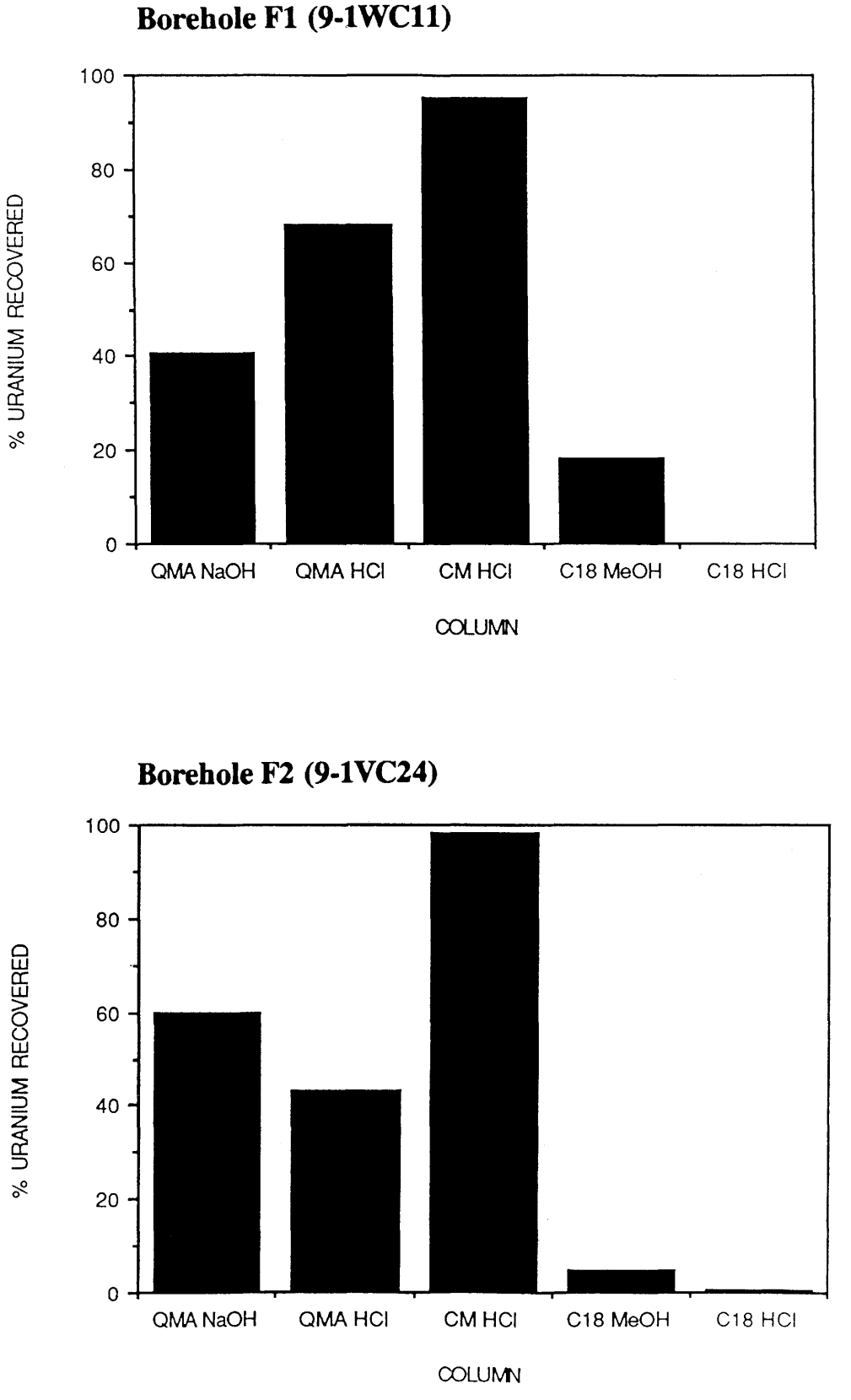

Figure 3-1. The percentage of uranium eluted from each column.

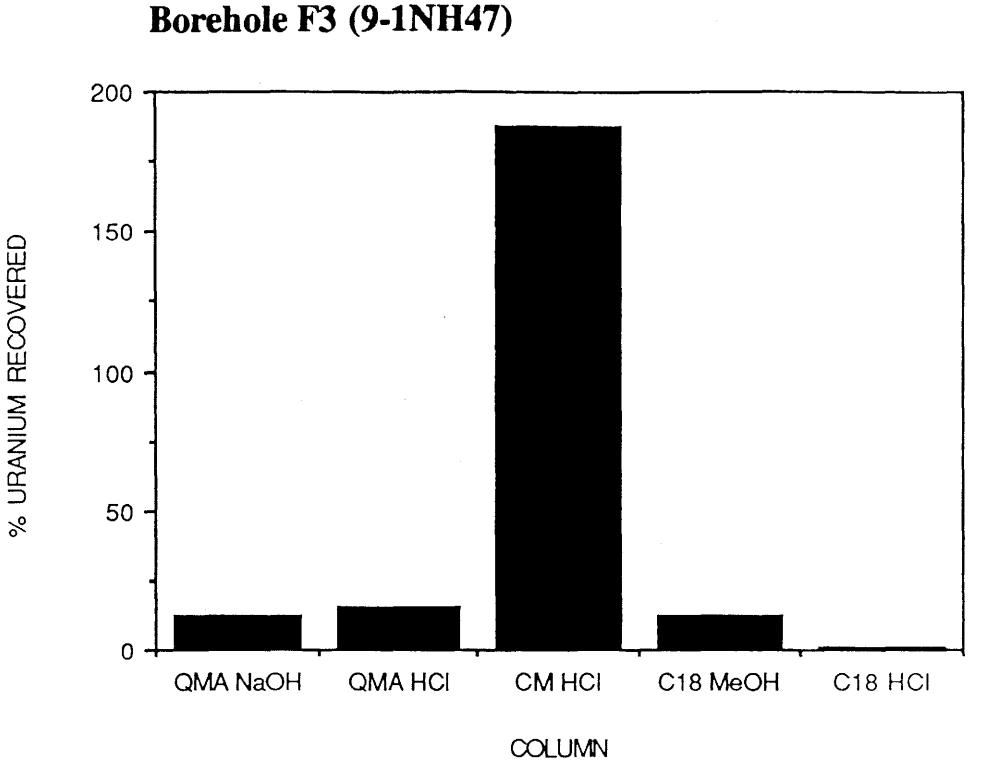

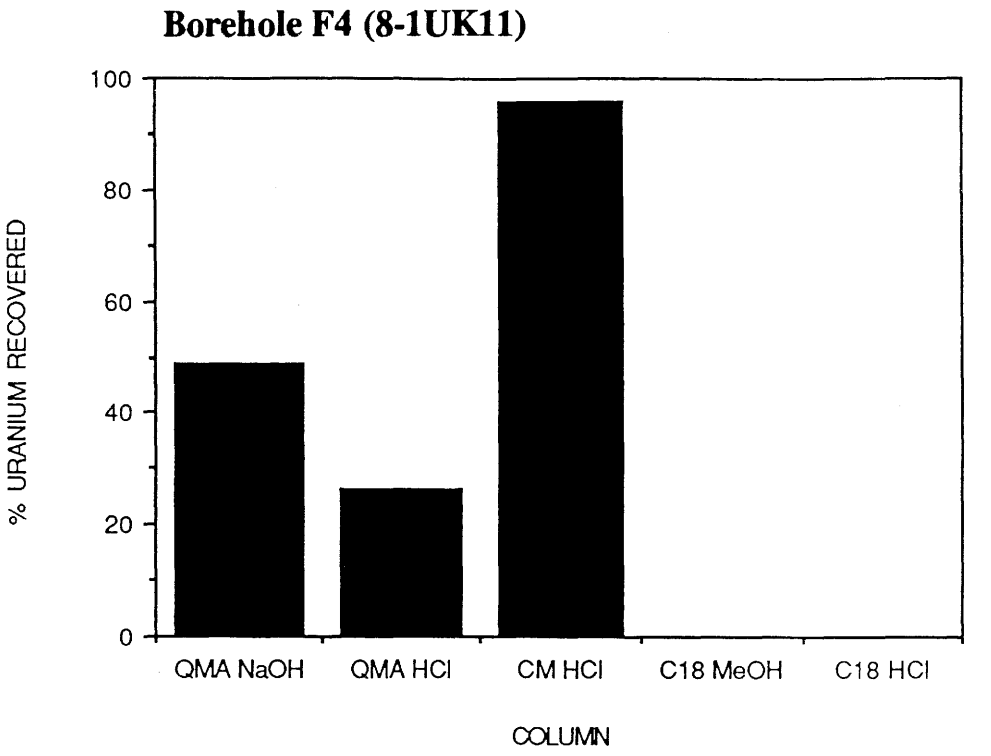

Figure 3-1 (contd.).

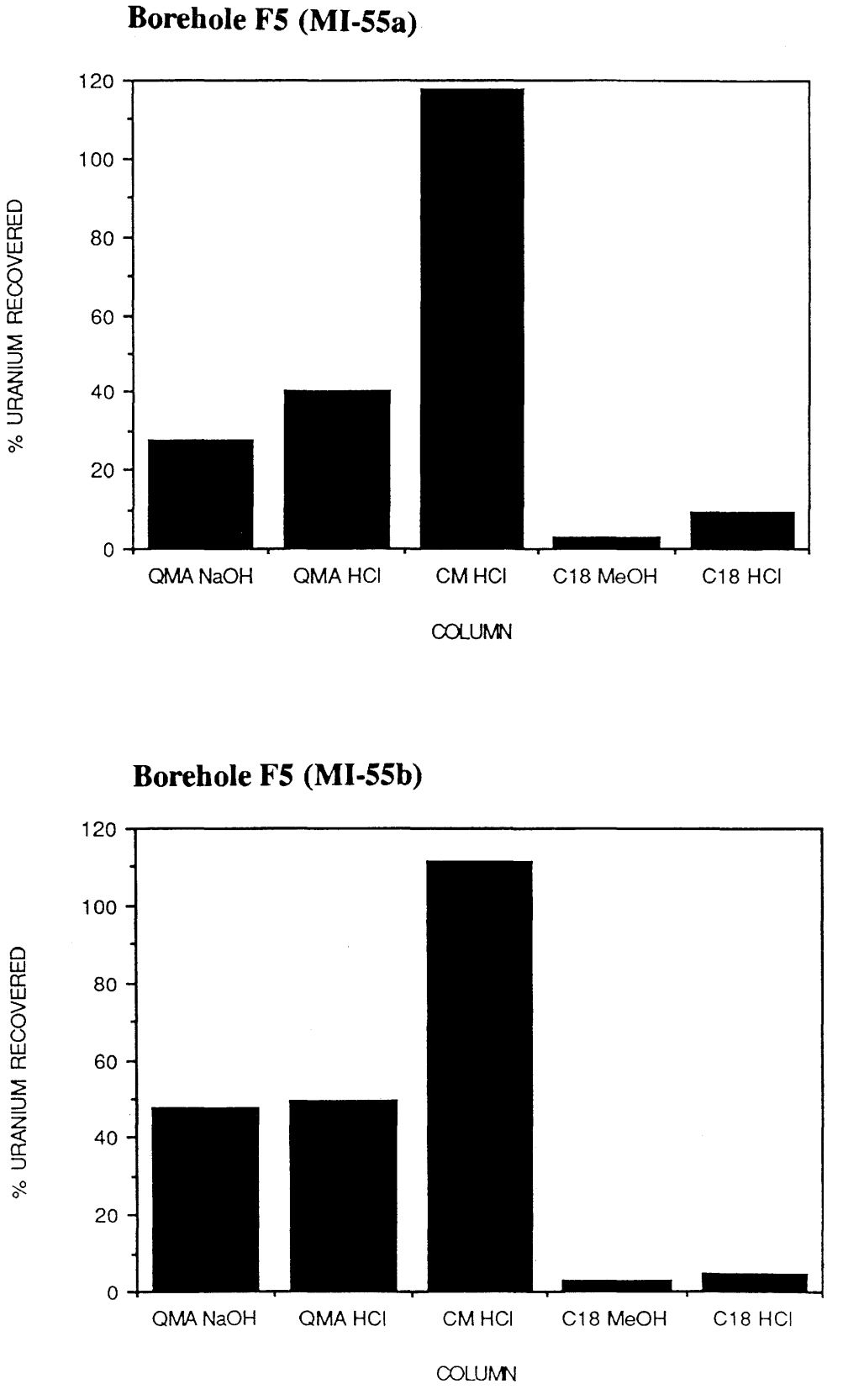

Figure 3-1 (contd.).

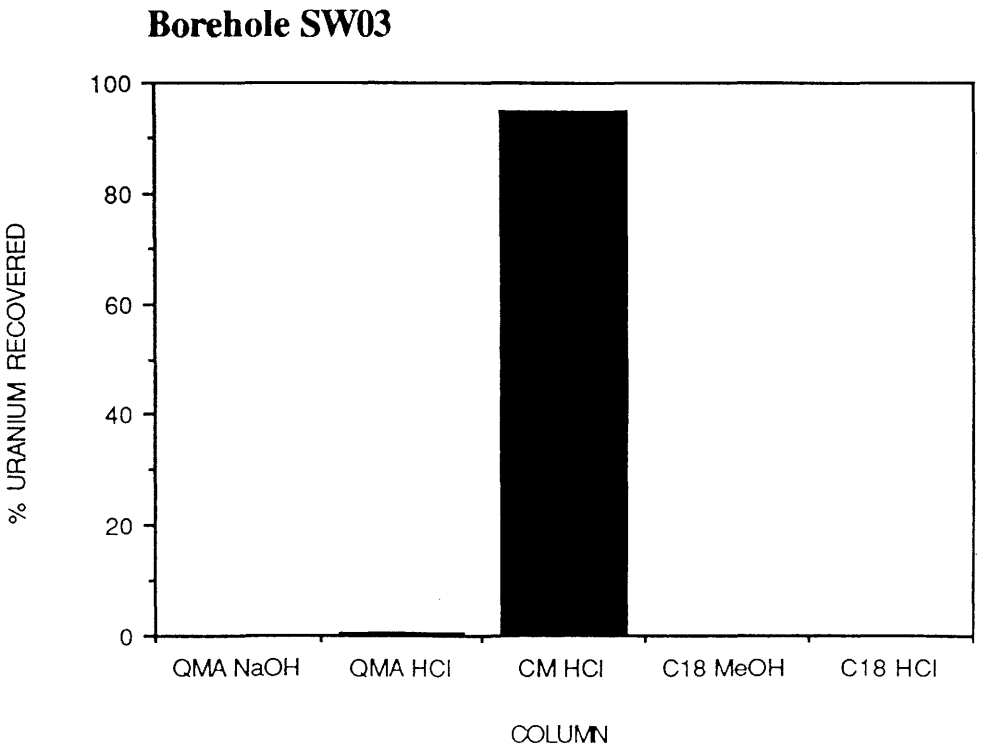

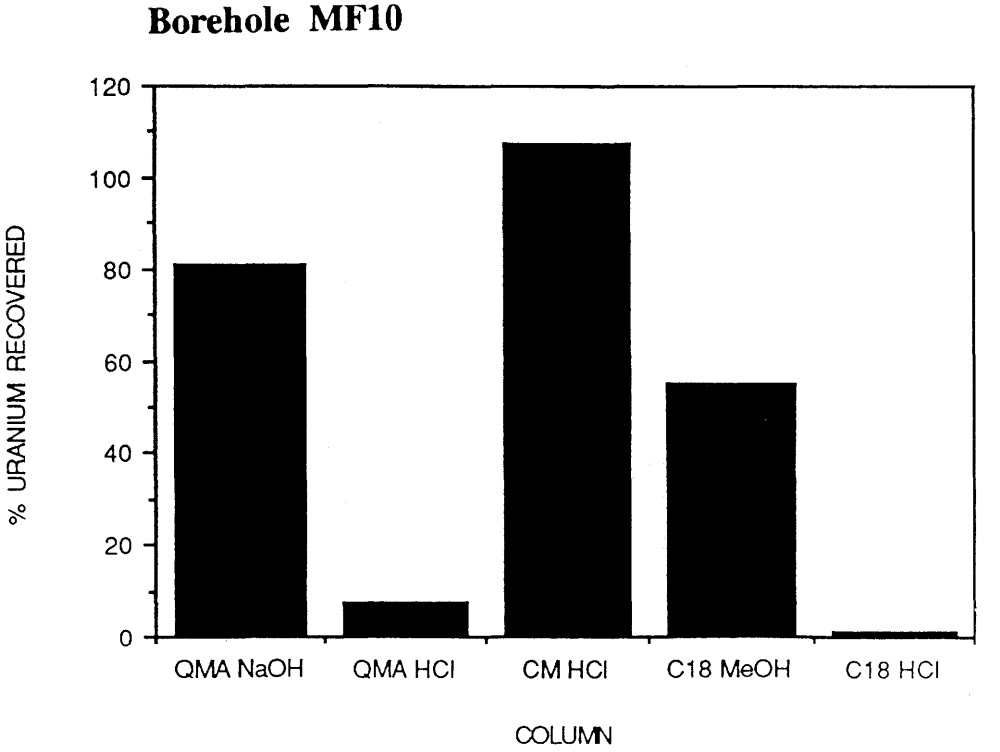

Figure 3-1 (contd.).

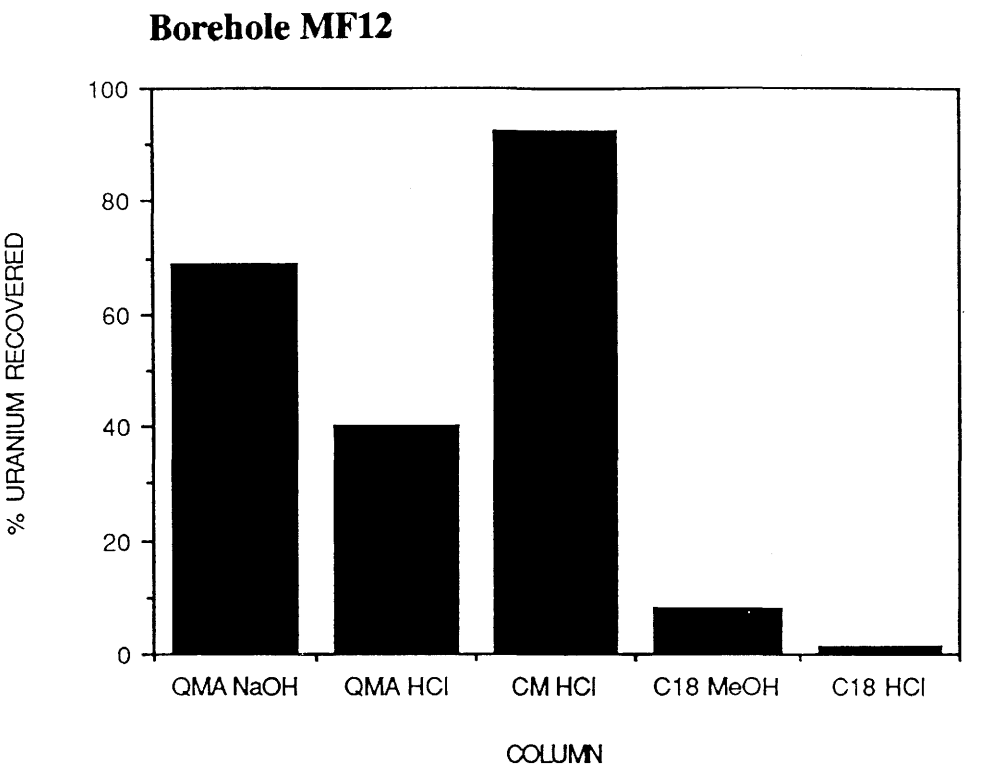

Figure 3-1 (contd.).

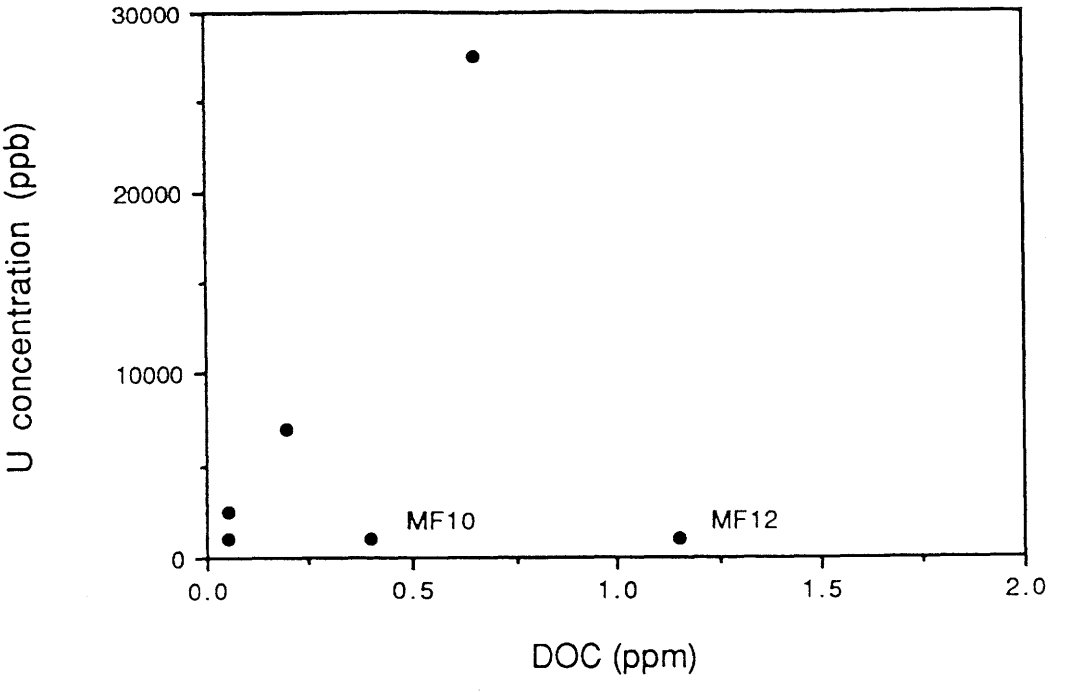

a.

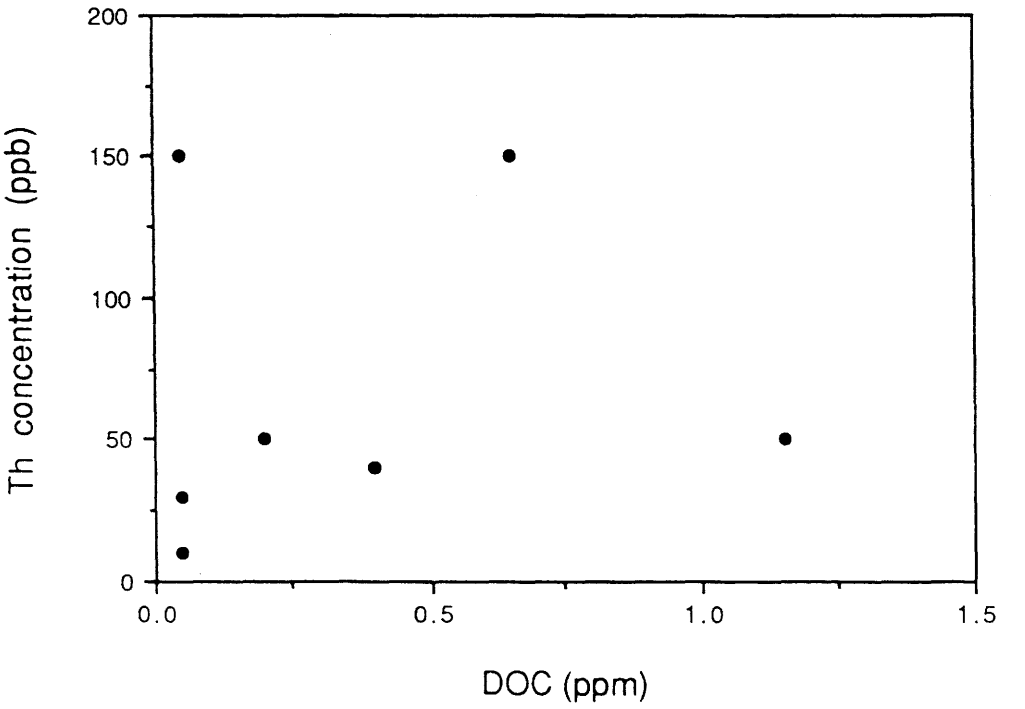

b.

Figure 3-2. (a) Uranium versus DOC and (b) thorium versus DOC.

Only small amounts of iron, aluminium and manganese are retained by the columns, but these amounts vary enormously (Table 3-II). Iron can be found associated with cationic species in all the columns, with the biggest percentage held by the CM column, while manganese is only retained in significant amounts by the CM column. Aluminium was found in all the columns but larger quantities were associated with cationic species. Samples with higher levels of uranium do not always show higher levels of iron; if time permitted, uranium levels should be compared with those of other elements to see if any relationship exists. However, studies of the exact nature of the iron colloids could indicate that only a small proportion of the total iron is of a form suitable for binding uranium.

A study of Table 3-III shows that some results do not tally, with more tracer being found in the eluates than in the total amount passed through the column. There are a number of factors which might cause this to happen. Some results are close to the detection limit and when multiplied by a factor, small variations are enhanced. The dilution of samples could also give rise to this problem. Passing more water through the columns might help eliminate detection limit problems but is, of course, more time-consuming. It is possible that different species are inhomogeneously distributed throughout the water and artifacts could be introduced by passing water through the columns.

It was thought that some iron species might be soluble in NaOH but the low iron levels for the NaOH eluate of the QMA column suggest that, at this site, this is not an added complication.

TABLE 3-III
Results showing the reproducibility of retention behaviour of the columns.

	U		Th	Fe	Al	Mn
	μg	ng	ng	ng	μg	μg
Borehole F2 (9-1VC24)						
Amount passed through		2500	10	810	25	119
Amount recovered:						
QMAa – NaOH	2.4	1500	<0.3	3	16	<0.12
– HCl		1075	5	39	99	<0.10
QMAb – NaOH	1.8	1020	<0.3	16	22	<0.10
– HCl		1625	5	25	91	<0.10
Borehole F4 (8-1UK11)						
Amount passed through		27,500	150	1470	895	1455
Amount recovered:						
OMAa – NaOH	13.8	13,380	<0.3	2	29	<0.12
– HCl	6.5	7300	<0.25	27	116	0.15
QMAb – NaOH	9.9	10,200	<0.3	0.8	13	<0.12
– HCl	8.8	9000	<0.25	19	101	0.15
CMa	26.3	nd	<5	97	137	503
CMb		22.5	<.25	41	65	465
Borehole MF12						
Amount passed through		1000	50	510	475	540
Amount recovered:						
OMAa – NaOH		690	<0.3	10	30	<0.12
– HCl		400	12.5	260	91	0.45
QMAb – NaOH		900	<0.3	16	22	<0.12
– HCl		300	5	151	81	0.83

8. Conclusions

The main conclusions to be drawn from this work are:

1. A large percentage of uranium in samples from the Osamu Utsumi mine has been retained by the CM column.
2. Some samples from this site also have a considerable amount of uranium retained by the QMA column.
3. At this site there appears to be a relationship between DOC and uranium.
4. Where detectable, thorium is mainly associated with cationic sites.

5. In samples from Morro do Ferro a large percentage of uranium is retained by the CM column, although both the QMA and C_{18} columns retain considerable amounts.

6. Where detectable, thorium is associated with cationic sites.

7. The CM column seems to be a very effective way of retaining uranium and the use of this column to collect and preconcentrate uranium for other techniques, apart from speciation experiments, should be considered.

9. Acknowledgements

The help of Ruy Frayha and his assistants Paulinho Rabelo and Serginho Scassiotti during sampling of the groundwaters is gratefully acknowledged.

The author also wishes to thank Dr. M. Cave (BGS) for analysing the solutions by ICP-AES and ICP-MS, Mr. D. Peachey (BGS) for his critical advice on the manuscript and Mr. B. Smith (BGS) for his constructive advice in the design of the equipment, his advice and comments on the manuscript and his preparation of the diagrams.

10. References

Breward, N. and Peachey, D., 1988. The development of portable equipment to study physical and chemical phases in natural water. *Rep. Brit. Geol. Surv.*. WE/88/25.

James, R.O. and Parks, G.A., 1982. In: E. Matijevic (Editor). Characterization of aqueous colloids by their electrical double-layer and intrinsic surface chemical properties. Surface and Colloid Science, 12. *Plenum Press*, New York.

Mantoura, R.F.C. and Riley, J.P., 1975. The analytical concentration of humic substances from natural waters. *Analytica Chemica Acta*, 76, 97-106.

Miles, C.J., Tuschall Jr., J.R. and Brezonik, P.L., 1983. Isolation of aquatic humus with diethylaminoethylcellulose. *Anal. Chem.*, 55, 410-411.

Smith, B., Stuart, M.E., Vickers, B.P. and Peachey, D., 1989. Characterisation of organics from the natural analogue site at Broubster, Caithness, Scotland. *Dep. Environ. Rep.* (DOE/RW/89.062), London, U.K.. (In preparation).

Tuschall Jr., J.B., Miles, C.J. and Brezonik, P.L., 1985. Efficiency of isolating humus from natural waters using DEAE cellulose. *Org. Geochem.*, 8(1), 137-139.